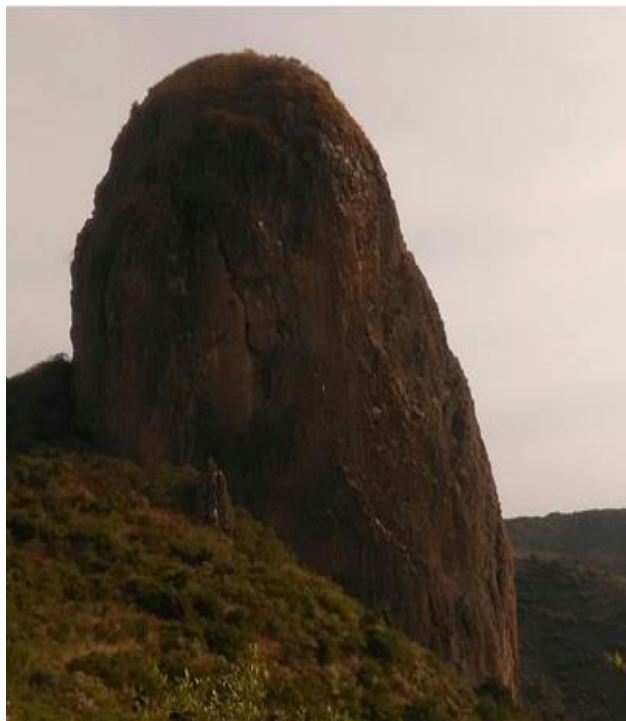


**Petrogenesis of Volcanic Plugs and Volcanic Rocks  
of the Infranz Area, Northwestern Ethiopia**

**Gedefaw Tadele**

**A Thesis Submitted to  
School of Earth Sciences**



**Presented in Partial Fulfillment of the Requirements for the  
Degree of Masters of Sciences in Geological science  
(Geochemistry)**



**ADDIS ABABA UNIVERSITY**

**Addis Ababa, Ethiopia**

**June, 2018**

**Petrogenesis of Volcanic Plugs and Volcanic Rocks  
of the Infranz Area, Northwestern Ethiopia**

**Gedefaw Tadele**

**A Thesis Submitted to  
School of Earth Sciences**

**Presented in Partial Fulfillment of the Requirements for the  
Degree of Masters of Sciences in Geological science  
(Geochemistry)**



**ADDIS ABABA UNIVERSITY**

**Addis Ababa, Ethiopia**

**June, 2018**

**Signature Page**

**Addis Ababa University**  
**School of Graduate Studies**

This is to certify that the thesis prepared by **Gedefaw Tadele**, entitled: *Petrogenesis of Volcanic Plugs and Volcanic rocks of the Infranz Area, Northwestern Ethiopia* and submitted in partial fulfillment of the requirements for the Degree of Master of Sciences in Geological science (Geochemistry) complies with the regulations of the University and meets the accepted standards with respect to originality and quality.

**Signed by the Examining Committee:**

**Advisor: Pro. Dereje Ayalew**      Signature \_\_\_\_\_ Date \_\_\_\_\_

**Examiner: Dr. Mulugeta Alene**      Signature \_\_\_\_\_ Date \_\_\_\_\_

**Examiner: Pro. Gezahegn Yirgu**      Signature \_\_\_\_\_ Date \_\_\_\_\_

---

**Chair of School or Graduate Program Coordinator**

## **Declaration of Originality**

I hereby declare that this is my original work prepared for the partial fulfillment of the Degree of Master of Science in the School of Earth Sciences, Addis Ababa University during 2018 under the supervision of **Prof. Dereje Ayalew**. Moreover, I am assuring that this work is not presented and published anywhere else. All sources are well referenced and acknowledged.

**Gedefaw Tadele**                      Signature \_\_\_\_\_ date \_\_\_\_\_

I hereby declare that this is his original work as part of his Master of Science in Geological Sciences (Geochemistry).

**Pro. Dereje Ayalew**                      Signature \_\_\_\_\_ date \_\_\_\_\_  
**Advisor**

## **ACKNOWLEDGMENT**

First of all, I would like to thank ‘Almighty God’ with his virgin mother holy of holies, Madonna, who made it possible to begin and finish this work successfully.

I would like to thank so much to the Gondar and Addis Ababa universities for providing me the opportunity and necessary support to pursue my masters study.

I would like to express my deepest gratitude to the learned Prof. Dereje Ayalew, my Advisor, for his real genuine and endless support from the beginning to the final completion of the thesis.

Words can’t express my feelings which I have for my parents and the whole family. I am highly indebted to them for their advice, encouragement and support.

My special thanks also go to my colleagues and friends for their great support and helpful suggestions.

Last but not least, thanks are also extended to the community of Infranz town for their impressive support during field work.

## TABLE OF CONTENTS

<b>Contents</b>	<b>Page No</b>
ACKNOWLEDGMENT	I
TABLE OF CONTENTS	II
LIST OF FIGURES	IV
LIST OF TABLE	V
ABSTRACT	VI
<b>CHAPTER ONE</b>	<b>1</b>
1. INTRODUCTION	1
1.1. Background Information	1
1.2. Statement of the problem	2
1.3. Significance of the Research	3
1.4. Location and Accessibility	4
1.5. Physiography and Climate	5
1.6. Objectives of the Study	6
1.6.1. General Objective	6
1.6.2. Specific Objectives	6
<b>CHAPTER TWO</b>	<b>7</b>
2. REGIONAL GEOLOGY	7
2.1. Introduction	7
2.2. Subdivision of the Northwestern Ethiopian Volcanic Province	8
2.2.1. The Oligo-Miocene Flood Volcanics	9
2.2.2. Mio-Pliocene Volcanics	12
2.2.3. Quaternary Volcanics	13
2.2.4. Volcanic Plugs	13
2.3. Genesis and Evolution of the Northwestern Ethiopian Volcanic Province	15
<b>CHAPTER THREE</b>	<b>17</b>
3. METHODOLOGY	17
3.1. Revision of Previous Works and Related Topics	17
3.2. Field Work	19
3.2.1. Sampling	19
3.3. Petrographic Analysis	20
3.4. Geochemical Analysis	20
<b>CHAPTER FOUR</b>	<b>22</b>
4. FIELD DESCRIPTION AND PETROGRAPHY	22
4.1. Field Description	22

4.2. Petrography	30
<b>CHAPTER FIVE</b>	37
5. RESULT OF GEOCHEMICAL ANALYSIS	37
5.1. Major Elements	37
5.2. Trace Elements	45
<b>CHAPTER SIX</b>	53
6. DISCUSSION	53
6.1. Field, Petrography and Geochemistry	53
6.2. Source Relations	54
6.3. Petrogenetic Processes	55
6.4. Comparison of Infranz and Previously Studied Volcanic Plugs	57
<b>CHAPTER SEVEN</b>	60
7. CONCLUSION AND RECOMMENDATION	60
7.1. Conclusion	60
7.2. Recommendation	61
<b>REFERENCES</b>	62
<b>APPENDIX I</b>	68
SECONDARY GEOCHEMICAL DATA	68
<b>APPENDIX II</b>	70
ABBREVIATIONS	70

## LIST OF FIGURES

<b>Figure</b>	<b>Page No</b>
Figure 1.1 Location map of the study area	4
Figure 1.2 Physiographic map of the study area	5
Figure 2.1 Impinging of the Afar mantle plume beneath Afro-Arabian lithosphere	7
Figure 2.2 Simplified geological map of the northern Ethiopian volcanic province	11
Figure 2.3 The possible ways of formation of Adwa volcanic plugs	14
Figure 3.1 The relative location of previous studies on volcanic plugs	18
Figure 3.2 Generalized summary of the methodological procedure	21
Figure 4.1 Geological map of the study area with sample locations	23
Figure 4.2 Field and outcrop photograph of the plug Molalit	24
Figure 4.3 Field and outcrop photograph of the plug Mender Mariam	25
Figure 4.4 Field and outcrop photograph of the plug Dur-Amba	26
Figure 4.5 Field and outcrop photograph of the plug Woyni-Amba	27
Figure 4.6 Field and outcrop photograph of the plug Koma	27
Figure 4.7 Field and outcrop photograph of the plug Asiba	28
Figure 4.8 Field and outcrop photograph of the plug Sebaha	29
Figure 4.9 Field and outcrop photograph of the plug Chalmut	29
Figure 4.10 Thin section microphotograph of VP1-NG (from Molalit)	31
Figure 4.11 Thin section microphotograph of VP2-NG (from Mender Mariam)	31
Figure 4.12 Thin section microphotograph of VP3-NG (from Dur-Amba)	32
Figure 4.13 Thin section microphotograph of VP4-NG (from Woyni-Amba)	33
Figure 4.14 Thin section microphotograph of VP5-NG (from Koma)	34
Figure 4.15 Thin section microphotograph of VP6-NG (from Asiba)	34
Figure 4.16 Thin section microphotograph of VP1-SG (from Sebaha)	36
Figure 4.17 Thin section microphotograph of VP2-SG (from Chalmut)	36
Figure 5.1 Total alkali (Na <sub>2</sub> O+K <sub>2</sub> O) versus silica (SiO <sub>2</sub> ) variation diagram	41
Figure 5.2 Major element oxides versus silica variation diagram	43
Figure 5.3 Incompatible trace element versus silica variation diagram	46
Figure 5.4 Trace element- element and trace element- trace element ratio diagram	48
Figure 5.5 Chondrite-normalized REE plots	50
Figure 5.6 Primitive mantle normalized incompatible, multi-element plots	52
Figure 6.1 TiO <sub>2</sub> versus SiO <sub>2</sub> diagram for the northern and northwestern Ethiopian plugs	58
Figure 6.2 Trace element-element and Trace element ratio-ratio diagrams for the northern and northwestern Ethiopian volcanic plugs.	59

**LIST OF TABLE**

<b>Table</b>		<b>Page No</b>
Table 5.1	Major and trace element geochemical analysis result	38

## **ABSTRACT**

The bi-modal basalt-rhyolite Ethiopian continental flood basalt, formed by the impingement of the Afar mantle plume beneath the Ethiopian lithosphere, contains a number of vertically sided, thought to be feeders of volcanic rocks at the time of their formation, volcanic plugs. Whole-rock major- and trace-element data including REEs are presented for volcanic plugs of the Infranz area, northwestern Ethiopia in order to investigate the petrogenesis of volcanic plugs and to understand petrogenetic inter-plug relationships. The geochemically phonolite-trachyte-rhyolite alkaline volcanic plugs of the Infranz area, are mostly characterized by nepheline, alkali feldspar and quartz phenocrysts respectively, set in dominantly alkali feldspar microlites of parallelly aligned groundmass that form typical trachytic texture. The Infranz volcanic plugs have almost similar major- and trace-element concentrations on the major-element oxide and trace-element versus silica variation diagrams hence, formed by the little role of fractional crystallization between them. These volcanic plugs on chondrite-normalized REE patterns show highly fractionated  $[La/Y]_N$  ( 8.97-21.66) REEs with negative Eu ( $Eu/Eu^* = 0.43-0.83$ ) anomalies; on the primitive mantle-normalized multi-element plots they illustrate negative anomalies in: Ba, Sr, P, and Ti. They are formed from the same, explained by the well- defined trends incompatible elements form, by the almost similar Zr/Nb, Zr/Th ratios they have, garnet free, shown by the greater than 10 x chondrites of sample/chondrite ratios, source formed by the same, illustrated by parallel to subparallel chondrite-normalized REE patterns, petrogenetic processes.

The variations in concentration of major elements (TiO<sub>2</sub>, Fe<sub>2</sub>O<sub>3</sub>, Al<sub>2</sub>O<sub>3</sub>, Na<sub>2</sub>O), trace elements (Nb, Th, Y) and incompatible trace element ratios (Zr/Th, Zr/Nb) between the Infranz volcanic plugs and Lima Limo rhyolites demonstrates the heterogeneity of their source. This implies that the Lima Limo rhyolites are not the fed products of the Infranz volcanic plugs.

*Key words:*

Infranz Volcanic plugs

Alkali feldspar

Geochemistry

## **HAPTER ONE**

### **1. INTRODUCTION**

#### **1.1. Background Information**

Ethiopia, the only place in the world where continental lithosphere is splitting and the beginning stage of sea–floor spreading can be seen on land (Williams, 2016), contains one of the youngest continental flood basalt province on earth formed by the impingement of the Afar mantle plume beneath the Ethiopian lithosphere (Marty et al., 1996; Beccaluva et al., 2009; Dereje Ayalew et al., 2002). Volcanism was started 45 Ma in southern (Davidson, 1980; George et al., 1998; Ebinger et al., 1993) and 30 Ma in northern Ethiopia (Hofmann et al., 1997; Kieffer et al., 2004; Dereje Ayalew et al., 2002). The formation of Oligocene, pre-rift Ethiopian continental flood basalt was followed by the central type Mio-Pliocene shield volcanoes, like Simien (30Ma), Gugufu, and Choke (22Ma) and Guna, 10.7 Ma (Kieffer et al., 2004). On Plio- Quaternary, volcanism then continued to occur: on the plateaus, best exemplified by the Tana volcanics (e.g. Prave et al., 2016), along the main Ethiopian rift (e.g. Rooney et al., 2012; Daniel, 2009) and along the afar rift, best exemplified by the Erta ale, Afar, Ethiopia. The focus lacking Ethiopian volcanic plugs, have no any well constrained ages other than the one by Natali et al. (2013) to talk about their history of volcanism parallely with the Ethiopian continental flood basalt. Even though most researchers agree that the northern and northwestern Ethiopian volcanic plugs are of quaternary (e.g. Daniel Meshesha and Shinjo, 2007; Miruts Hagos et al., 2010), Mio-Pliocene (e.g. Beyth, 1972) age formed probably by tilting and updoming of the surrounding rocks (Kazmin, 1975), Natali et al. (2013) constrain the age of Adwa volcanic plugs to be 19-15 Ma.

The Ethiopian continental flood basalt (CFB) province is subdivided in to three major geographical and geomorphological parts: the Ethiopian plateaus (northwestern, southwestern and southeastern), the main Ethiopian rift and the Afar rift (Kazmin, 1979; Berhe et al., 1987; Hart et al., 1989). The northwestern branch of the Ethiopian continental flood basalt sequence, based on chrono-stratigraphy, is classified as: the Ashange, Aiba, Alaje and termaber (Megezez and Gussa) formations (Merla et al., 1979; Berhe et al., 1987;

Mengesha Tefera et al., 1996). But, latter on from field observations combined with the petrological characteristics of the lavas, Pik et al. (1998) conclude that the above classification is not valid for the whole northwestern Ethiopian plateau, rather broadly the province is classified geographically as high TiO<sub>2</sub> and low TiO<sub>2</sub> Sub- Provinces. The plateau rhyolites are geographically correlated with the basalts, low- and high-TiO<sub>2</sub> rhyolites occurring in association with low- and high-TiO<sub>2</sub> flood basalts (Dereje Ayalew et al., 2002; Dereje Ayalew and Gezahegn Yirgu, 2003).

According to Gates and Ritchie (2007), volcanic plugs are tower like landforms consisting of an igneous core of an extinct volcano whose outer layers have eroded away; the neck is composed of magma that has crystallized in the conduit of the volcano. They form (<https://pubs.usgs.gov/gip/volc/structures.html>), when congealed magma, along with fragmental volcanic and wall rock materials are preserved in the feeding conduits of volcanoes upon cessation of feeding activity. These towerlike, conspicuous features of volcanic landforms, volcanic plugs, are observed around Infranz (the present study area), northwestern Ethiopia, and no detailed work is conducted as a whole Ethiopia and particularly at the study area. This research is aimed to study the petrogenesis of volcanic plugs and to understand inter-plug petrogenetic relationships with the help of field observation, petrographic studies from thin section and rock geochemistry by using geochemical analysis. Since volcanic plugs are thought to be the feeders of the surrounding volcanic rocks, their relationships with the northwestern Ethiopian felsic volcanic rocks are also studied with the in light of new, taken from Infranz volcanic plugs, and existing, taken from Lima Limo rhyolites studied by Dereje Ayalew and Gezahegn Yirgu (2003), geochemical data.

## **1.2. Statement of the Problem**

Numerous researches have been conducted on the Ethiopian continental flood basalt, including the northwestern Ethiopian volcanic sub-province. Most of the studies on the northwestern Ethiopian plateau have focused on basalts (e.g. Pik et al., 1998; 1999; Becaluva et al., 2009), rhyolites and ignimbrites (e.g. Dereje Ayalew et al., 2002; Dereje Ayalew and Gezahegn Yirgu, 2003). Very little is known about the petrogenetic inter-plug and plug-felsic volcanic rock relationships of the northwestern Ethiopian volcanic plugs despite an interesting geological idea that, volcanic plugs are the feeders of the surrounding volcanic rocks (<https://pubs.usgs.gov/gip/volc/structures.html>) formed when

their feeding activity is ceased. Dercq et al. (2001) investigated the genesis of northwestern Ethiopian volcanic plugs and their relationship with the felsic volcanic rocks but, because of it is not only somewhat regional so that, they didn't take any sample from the present study volcanic plugs but also, they rely only on by three volcanic plugs to justify the feeding nature of those volcanic plugs for the northwestern Ethiopian felsic volcanic rocks, which is not representative. These authors documented that, from the three volcanic plugs included under their study, the southern plug, located around Debre Tabor, had a different crystallization history; the northwestern Ethiopian volcanic plugs are not the feeders of trap volcanism rather for trachytes in shield volcanoes.

Therefore, the presence of adequate volcanic plugs to include as much volcanic plugs as necessary combined with the absence of detailed work on their petrogenesis, petrogenetic inter-plug and plug-felsic volcanic rock relationships, raises a question of investigating the petrogenesis of volcanic plugs and understanding petrogenetic inter-plug and plug-felsic volcanic rock relationships. This study mainly focuses on investigation of petrogenesis of volcanic plugs and petrogenetic inter-plug relationships of the Infranz volcanic plugs, northwestern Ethiopia with the help of field investigation, petrography and geochemical analysis. The relationships Infranz volcanic plugs, this study, have with the felsic volcanic rocks of northwestern Ethiopia with in the light of existing, Lima Limo rhyolites studied by Dereje Ayalew and Gezahegn Yirgu (2003) are also considered.

### **1.3. Significance of the Research**

Field observation, petrographic and geochemical analysis of samples from volcanic plugs provides important information on the relationship between volcanic plugs and felsic volcanic rocks. Basically, the result of this study has its own role for scientific community in that it shows the petrogenesis of volcanic plugs and fills the gap in understanding their relation with the felsic volcanic rocks of northwestern Ethiopia. Moreover, the geochemical data serves as a reference tool to understand the northwestern Ethiopian volcanic plugs which have no more data before. In addition to that, the geochemical and petrographic studies of those volcanic plugs will be used as a reference framework for the students, scientific community and other researchers after publication.

#### 1.4. Location and Accessibility

The study area is located around Infranz, Amhara region, northwestern Ethiopia. The area can be accessed by the major road connecting Addis Ababa to Bahirdar and to Gondar town. Geographically the area is approximately bounded between  $11^{\circ}49'00''$  to  $12^{\circ}26'00''$  N latitude and  $37^{\circ}27'00''$  to  $37^{\circ}57'00''$  E Longitude (Fig 1.1).

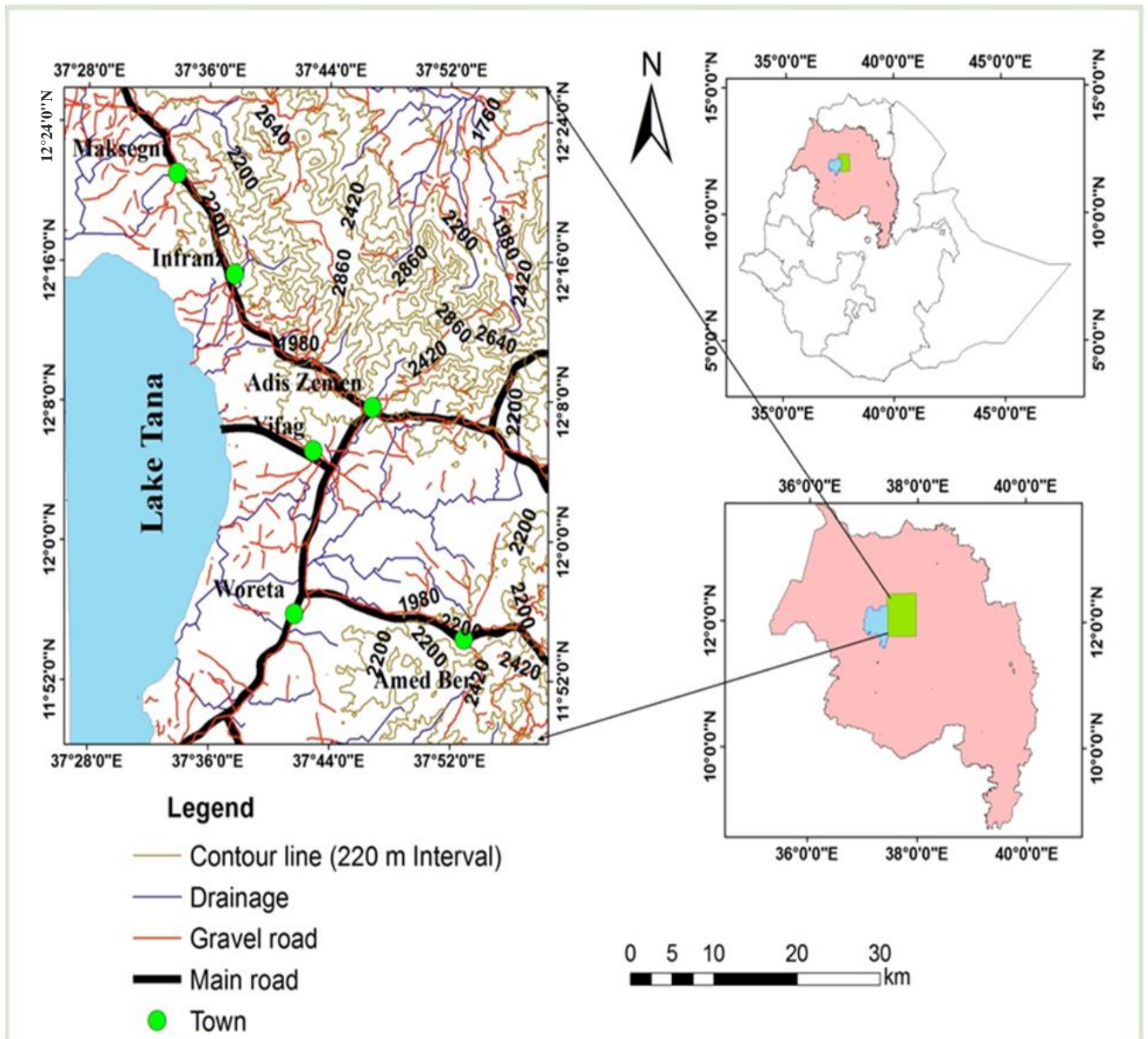


**Figure 1.1** Location map of the study area, around Infranz, northwestern Ethiopia.

### 1.5. Physiography and Climate

The study area, around Infranz, northwestern Ethiopia is characterized by both rugged and somewhat flat topographic features (Fig. 1.2). Most part of the study area is controlled by rugged topographic features on the northern, northeastern and southern part and also on the southern end. Flat topographic features are dominantly found on the south eastern and western part of the study area.

According to (<https://en.climate-data.org/location/1183/>), the study area around Infranz is characterized by mild generally warm and temperate. As documented in this cite the area is grouped under humid subtropical climate with the lowest precipitation in January on average 4mm whereas, the highest precipitation is in July on average 328mm. At an average temperature of 22.0 °C, April is the hottest month of the year; August is the coldest month, with temperatures averaging 17.6 °C.

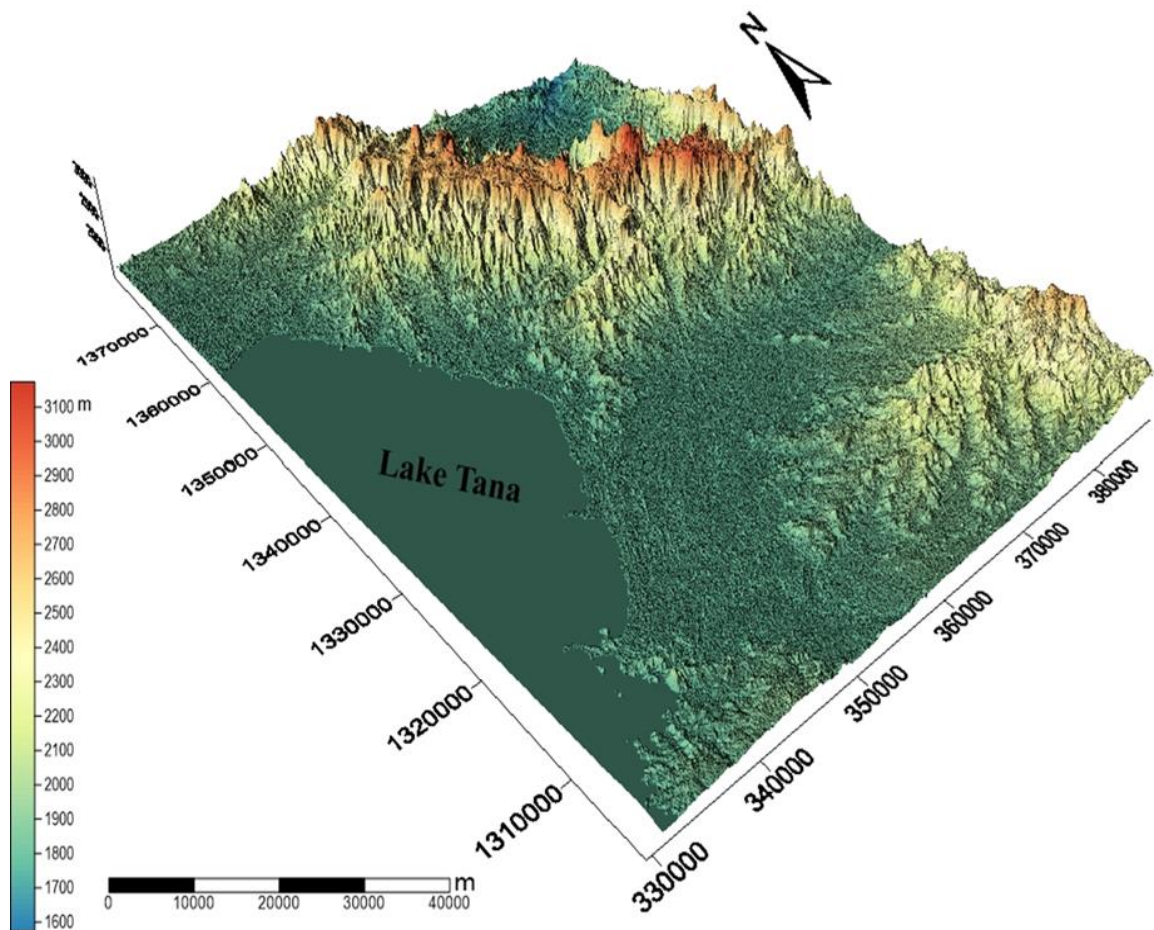


**Figure 1.2** Physiographic map of the study area, around Infranz, northwestern Ethiopia.

## **1.6. Objectives of the Study**

### **1.6.1. General Objective**

The foremost objective of this study is to investigate the petrogenesis of volcanic plugs of the Infranz area, northwestern Ethiopia and to understand petrogenetic inter-plug relationships.

### **1.6.2. Specific Objectives**

The specific objectives of this study are:

- To determine whether the Infranz volcanic plugs, northwestern Ethiopia are the feeders for the Lima Limo rhyolites or not.
- To understand major-and trace-element signatures of the volcanic plugs of the Infranz area, with the aim to know the source of magma.
- To know the processes involved in the evolution of magma that form the present Infranz volcanic plugs.
- To describe the petrography of volcanic plugs of the Infranz area in order to understand the mineralogical composition.

## CHAPTER TWO

### 2. REGIONAL GEOLOGY

#### 2.1. Introduction

The Ethiopian continental flood basalt (CFB) is thought to have formed by the impingement of the Afar mantle plume (Fig. 2.1) beneath the Ethiopian lithosphere (Beccaluva et al., 2009; Marty et al., 1996; Dereje Ayalew et al., 2002; Natali et al., 2011) and is associated with Africa–Arabia continental break-up (Hofmann et al., 1997; Pik et al., 1998; Kieffer et al., 2004). According to Berhe et al. (1987) the pre-rift, Oligocene Ethiopian –

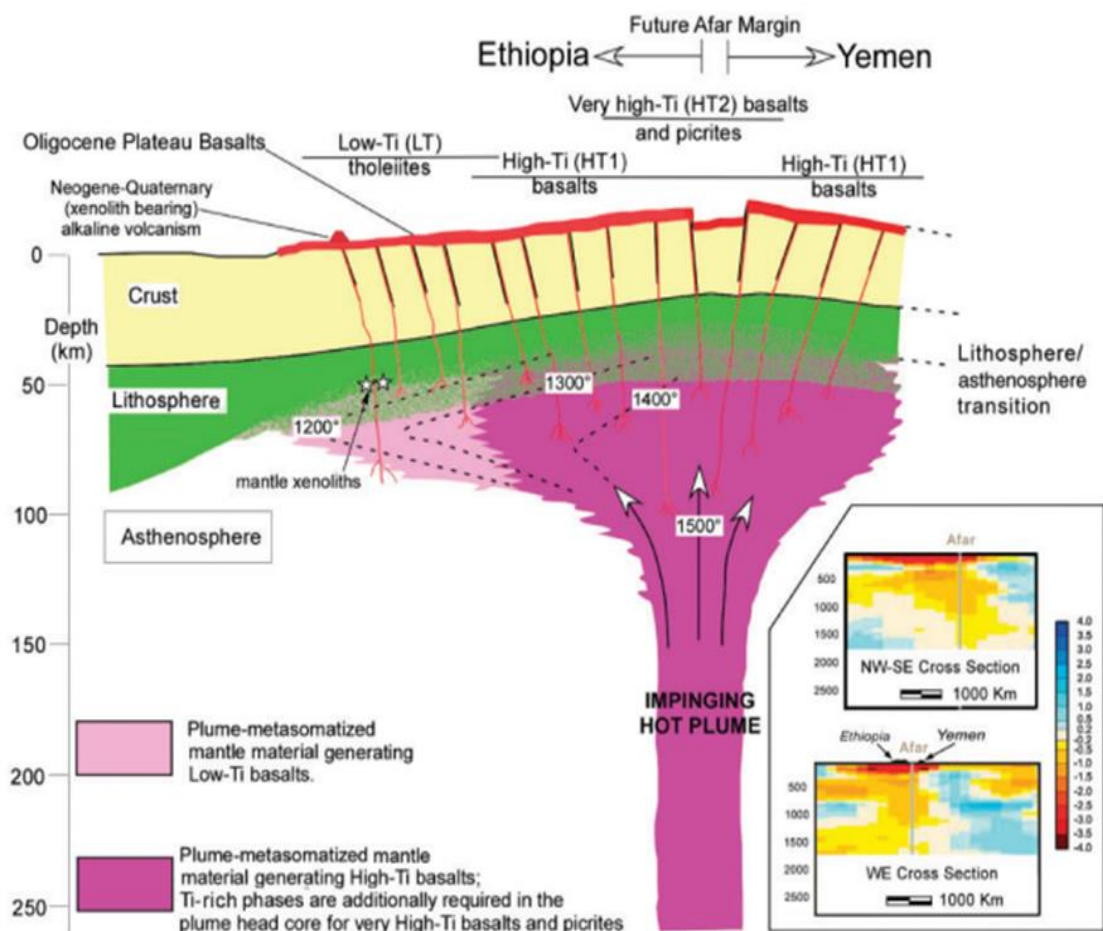


**Figure 2.1** Shows the impinging of the Afar mantle plume beneath the Afro-Arabian lithosphere that forms the Ethiopian and Yemen continental flood basalt, from Beccaluva et al. (2009).

continental flood basalt were emplaced in three major stages. Stage 1, mainly older than 40 Ma, stage 2, 40 to 30 Ma, and stage 3 spans from 30 to 21 Ma; the overlying shield volcanics of Ethiopia is considered as the fourth stage with an age spans of 7 to 25 Ma. This flood basalt forms the huge volume of lavas about  $3.5 \times 10^5 \text{ km}^3$  (Mohr, 1983), probably greater than  $1.2 \times 10^6 \text{ km}^3$  (Rochette et al., 1998); that form a pile on average up to 2 km thick (Berhe et al., 1987; Dereje Ayalew and Gezahegn Yirgu, 2003; Pik et al., 1998), and covers more than  $600,000 \text{ km}^2$  (Mohr and Zanettin, 1988). The province consists of rhyolitic and trachytic lavas and pyroclastic rocks that are interbedded with the flood basalts, particularly at upper stratigraphic levels; volume of the felsic rocks is estimated to be  $60000 \text{ km}^3$ , 20% of that of the trap volcanics (Dereje Ayalew et al., 2002). The Cenozoic Ethiopian continental flood volcanics contains bimodal basalt-rhyolite suit of rocks (e.g. Kieffer et al., 2004; Dereje Ayalew et al., 2002) and have erupted approximately 30 Ma ago, over a period of 1 Myr or less (Hofmann et al., 1997).

The Ethiopian continental flood basalt is subdivided in to three major geographical and geomorphological parts: the Ethiopian plateaus (northwestern, southwestern and southeastern), the main Ethiopian rift and the Afar rift (Kazmin, 1979; Daniel Meshesha and Shinjo, 2007; Berhe et al., 1987; Hart et al., 1989). Geochemical studies on each of these geographical and geomorphological parts; northwestern (e.g. Beccaluva et al., 2009; Minyahl Teferi et al., 2014), southwestern and southeastern (e.g. Dereje Ayalew et al., 2006; Rooney et al., 2017b;), main Ethiopian rift (e.g. Rooney et al., 2017a; Furman, 2017) and the Afar rift (e.g. Mulugeta Alene et al., 2017; Miruts Hagos et al., 2016) have conducted. From the Ethiopian geological map which was prepared by Merla et al. (1979) and from the explanation of geological map of Ethiopia by Mengesha Tefera et al. (1996), subdivisions of Ethiopian continental flood basalt has different nomenclature in different parts of the county. Subdivision of the northwestern Ethiopian continental flood basalt, by considering both the earlier and recent classifications, is given below.

## **2.2. Subdivision of the Northwestern Ethiopian Volcanic Province**

The northwestern Ethiopian continental flood basalt, according to the earlier classifications, is subdivided in to: Ashange basalt, Aiba basalt, Alaje rhyolite and the termaber (Gussan and Megezez) formations based on the stratigraphy (from oldest to youngest) and age of the formations (Merla et al., 1979; Mengesha Tefera et al., 1996; Berhe et al, 1987;

Mohr, 1983). But, latter on from field observations combined with the petrological characteristics of the lavas Pik et al. (1998) conclude that the above classification is not valid for the whole northwestern Ethiopian plateau. Rather the authors suggest another classification scheme for the province; despite their age difference, broadly in to high TiO<sub>2</sub> (HT) and low TiO<sub>2</sub> (LT) sub provinces (Fig. 2.2). There are three, 30 Ma magma types which construct the northern Ethiopian volcanic province, according to Keiffer et al, (2004) : the almost tholeiitic, low in incompatible element, flood basalts overlain by the same age and magmatic series of Simien shield, the thin layer of alkaline, moderate in incompatible element, flood basalt overlain by the same affinity 22 Ma shield volcanoes of Choke and Gugufu and the more magnesium, incompatible trace element enriched alkaline flood basalt overlain by, silica under saturated, young Guna shield volcano which have an age of 10.7 Ma.

According to the modern geological map of northern Ethiopian plateau (e.g. Pik et al., 1998; 1999; Dereje Ayalew, 2011; Dereje Ayalew and Gibson, 2009), the northern Ethiopian volcanics are classified in to three: Oligo- Miocene volcanics, Mio-Pliocene Volcanics and quaternary volcanics, based on absolute ages. The province also contains the conspicuous landforms, so called volcanic plugs (Miruts Hagos et al., 2010; Natali et al, 2013; Begosew Abate et al., 1998; Daniel Meshesha and Shinjo, 2007; Kazmin, 1975). Therefore, here the subdivision of the northwestern Ethiopian volcanic province is better classified based on the above absolute age scheme. The vertically sided land forms, volcanic plugs, of the northern Ethiopian plateau have no well-defined ages, though Natali et al. (2013) documented their age to be 15Ma; therefore volcanic plugs here are considered as the fourth part of the province in this subdivision.

### **2.2.1. The Oligo - Miocene flood volcanics**

Based on the traditional way of classification, the Oligocene flood volcanics or the pre-rift flood volcanics of the northern Ethiopian continental flood basalt are classified in to three formations (Berhe et al., 1987): the Ashange basalt, Aiba basalt and the Alaje ignimbritic units. Ashange basalt represents the earliest fissural flood basalt volcanism on the northwestern Ethiopian volcanic province. It consists of predominantly mildly alkaline basalts with interbedded pyroclastics and rare rhyolites (Mengesha Tefera et al., 1996) and rests conformably on arenaceous sediments and locally on basements (Merla et

al., 1979). The Ashange basalt is identified by its uniformly fractured and folded nature because of the huge Aiba flood basalt overlies it (Zanettin et al., 1978). Aiba basalt, which represents the second major pulse of fissural volcanism in northwestern Ethiopian plateau, is entirely composed of massive flood basalt flows, with and sometimes without intervening agglomerate beds. This basalt unconformably overlies the Ashange formation and show distinctive tholeiitic nature with transitions to mildly alkaline varieties (Mengesha Tefera et al., 1996). The average flows of the Aiba basalt ranges from 15 - 50 m thick and are generally composed of dense, dark, fine-grained olivine basalt, commonly columnar (Merla et al., 1979; MacDougall, 1988). The third part of the flood basalt formation, the Alaje formation, unconformably rests on Aiba basalts and in some places on the Mesozoic sediments. It mainly consists of aphyric flood basalts associated with rhyolites and subordinate trachytes (Mengesha Tefera et al., 1996). In Alaje formation, individual flows are up to tens of meters thick, and commonly include both welded and unwelded units (MacDougall, 1988). The basalts of Alaje formation are tholeiitic of the transitional type (Merla et al., 1979) and the acidic rocks are more alkaline, associated with sub-alkaline acidic members (Mengesha Tefera et al., 1996). The secession of the Oligocene flood basalt forms on average, a pile up to 2 km (Pik et al., 1998; Dereje Ayalew et al., 2002; Dereje Ayalew and Gezahegn Yirgu., 2003; Beccaluva et al., 2009; Hoffman et al., 1997) and overlies the Mesozoic sedimentary basement (e.g. in Simien mountain, Lalibela area) and the Precambrian crystalline basement (e.g. in the Adigrat area, west of Adigrat) (Merla et al., 1979; Beccaluva et al., 2009; Ukstins et al., 2002).

According to the Newly emerged, principally based on the TiO<sub>2</sub> concentration, classification of the northwestern Ethiopian volcanic province, the province is classified geographically as the high TiO<sub>2</sub> (HT) and low TiO<sub>2</sub> (LT) sub-province basalts (Pik et al., 1998; Beccaluva et al., 2009) and rhyolitic ignimbrites associated with those basalts (Dereje Ayalew et al., 2002). The High titanium group (HT2) suites exhibit high TiO<sub>2</sub> (2.6-5%) and low SiO<sub>2</sub> (44-4%), whereas the Low titanium group (LT) exhibits low TiO<sub>2</sub> (1-2.6%) and high SiO<sub>2</sub> (47-51%). Rhyolitic ignimbrites of the region which classified as low TiO<sub>2</sub> and high TiO<sub>2</sub> suits are characterized by TiO<sub>2</sub> (0.3-0.5%) and (0.5-1%) respectively (Dereje Ayalew and Gezahegn Yirgu, 2003). The high TiO<sub>2</sub> basalts are exposed on the eastern part of the northwestern Ethiopian province whereas, the low TiO<sub>2</sub> basalts are exposed on the northern part of the province (Pik et al., 1998); rhyolites also follow the same trend (Dereje Ayalew et al., 2002; Dereje Ayalew and Gezahegn Yirgu, 2003). Of

the three regionally distinct rhyolites identified by Dereje Ayalew and Gezahegn Yirgu (2003), Lima Limo and Wegel Tena rhyolites are found in the northwestern Ethiopian plateau.

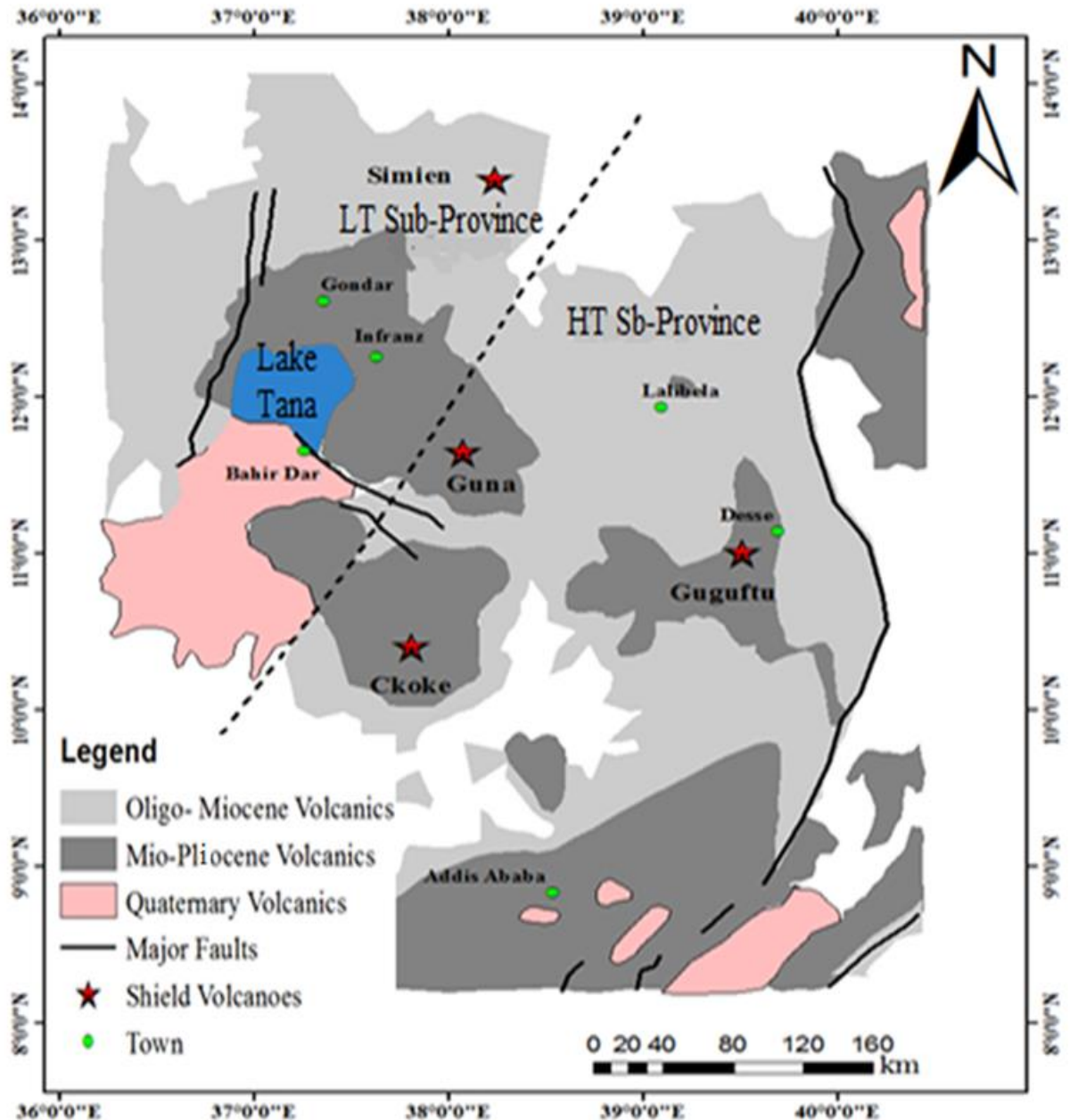


**Figure 2.2** Simplified geological map of the northwestern Ethiopian volcanic province (After, Kieffer et al., 2004). The dashed line shows the proposed boundary between high Ti and low Ti sub-provinces (from Pik et al., 1998). Note that, for simplicity and to append with the above subdivision of the northwestern Ethiopian volcanic province, sedimentary and metamorphic rocks are not shown here in the geological map.

### **2.2.2. Mio-Pliocene Volcanics**

According to Merla et al. (1979), Termaber basalts (shield group) were erupted from central volcanoes of Hawaiian type with still preserved edifices (e.g. Ras Dashen, Choke). Large amounts of tuffs, lenticular lava flows, scoriaceous lava flows and typical red paleosoils construct the termaber formation. In contrast to the pre-rift flood volcanics (Ashange, Aiba and Alaje), Termaber formation have alkaline affinity (Mengesha Tefera et al., 1996). Although smaller and steeper edifices occur, the mafic lavas comprising the Termaber formation are low angled shield, up to tens of kilometers in diameter (Macdougall, 1988).

The Oligocene basalts are overlain by the conspicuous, low-angle shield and less voluminous Miocene lavas erupted from large central volcanoes (Hoffman et al., 1997; Pik et al 1998; Keiffer et al., 2004). This the less voluminous overlying shield volcanics ages 7 to 25 Ma, according to Berhe et al. (1987), represents a localized terminal episode built on the plateau and are considered a fourth stage of volcanism. Even though there are no multiple researches done on the shield volcanoes of northwestern Ethiopian volcanic province, Kieffer et al. (2004) have conducted a detail investigation on the northwestern Ethiopian shield volcanoes. The composition of shield volcanoes of northwestern Ethiopia matches that of the underlying flood basalts and rhyolites (Kieffer et al. 2004). According to Kieffer et al. (2004) shield volcanoes contain lavas that are thinner and less continuous than the underlying flood basalts. The authors also documented the bimodal nature of the shield volcanoes like that of the flood volcanics and the presence of sequences of alternating basalts, rhyolitic and trachytic lava flows, tuffs and ignimbrites, particularly near their summits. Simien, Gugufu, Choke and Guna are considered as the main shield volcanoes which by the earlier researchers grouped under the Termaber formation. The base and the top of simien shield has an age of approximately 30 Ma (Kieffer et al., 2004; Rochette et al., 1998) and 18.7 Ma respectively (Kieffer et al., 2004) which is taken as the oldest shield compared to the other shield volcanoes of Gugufu and Choke with 22 Ma and Guna 10.7 Ma (Kieffer et al., 2004). Shield volcanoes farther to the south have ages between 20 and 3 Ma (Ukstinset al., 2002).

### **2.2.3. Quaternary Volcanics**

Despite their highest destitution along the main Ethiopian and Afar rift, the presence of Quaternary volcanic rocks (both basalts and felsic rocks) on the northwestern Ethiopian volcanic province are explained by different researchers at different times (e.g. Kazmin, 1975; Merla et al., 1979; Mengesha Tefera et al., 1996; Daniel Meshesha and Shinjo, 2007). Moreover, the Quaternary volcanics located south of Lake Tana are observed on the geological map of northern Ethiopian volcanic province (Fig. 2.2). According to Prave et al. (2016), the northwestern Ethiopian volcanic province around Lake Tana contains the Pre-rift flood basalts, thick and extensive felsic ignimbrites and rhyolites and localized scoriaceous basalts. The localized scoriaceous basalts have an  $^{40}\text{Ar}/^{39}\text{Ar}$  age of  $0.033 \pm 0.005/0.005$  Ma which is very young. The Quaternary volcanics of northwestern Ethiopia, emplaced south of Lake Tana, according to Daniel Meshesha and Shinjo (2007) also consists of single lava flows with pahoehoe structure and scoria cones. Petrographically basalts are characterized by olivine phenocrysts with minor plagioclase and clinopyroxene set in the holocrytalline groundmass whereas, scoria cones are characterized by poorly to moderately sorted loose grains ranging from lapilli –to-bomb – size; rock fragments of scoria cones are mainly olivine to olive- clinopyroxene phyric basalts and mantle xenoliths. According to Begosew et al. (1998) the Quaternary volcanics of Lake Tana, northwestern Ethiopia basalts are characterized by the phenocrysts of olivine, plagioclase, and clinopyroxene and in some cases nepheline in a fine grained groundmass.

### **2.2.4. Volcanic Plugs**

According to Gates and Ritchie (2007) definition of volcanic plugs, volcanic plugs/necks are towerlike landforms consisting of the igneous core of an extinct volcano whose outer layers have been eroded away; the neck is composed of magma that has crystallized in the conduit of the volcano. Williams (2016) clearly envisage the two possible ways of formation of Adwa volcanic plugs (Fig 2.3). According to her explanation, the volcanic plugs of Adwa are exposed either by the eroded away of volcanoes around them or by the pressure that pushed up below like a piston. The volcanic plugs of Adwa, northern Ethiopia, according to Williams (2016), which may also applied for the northwestern Ethiopian volcanic plugs follows the following steps in their formation (Fig 2.3):

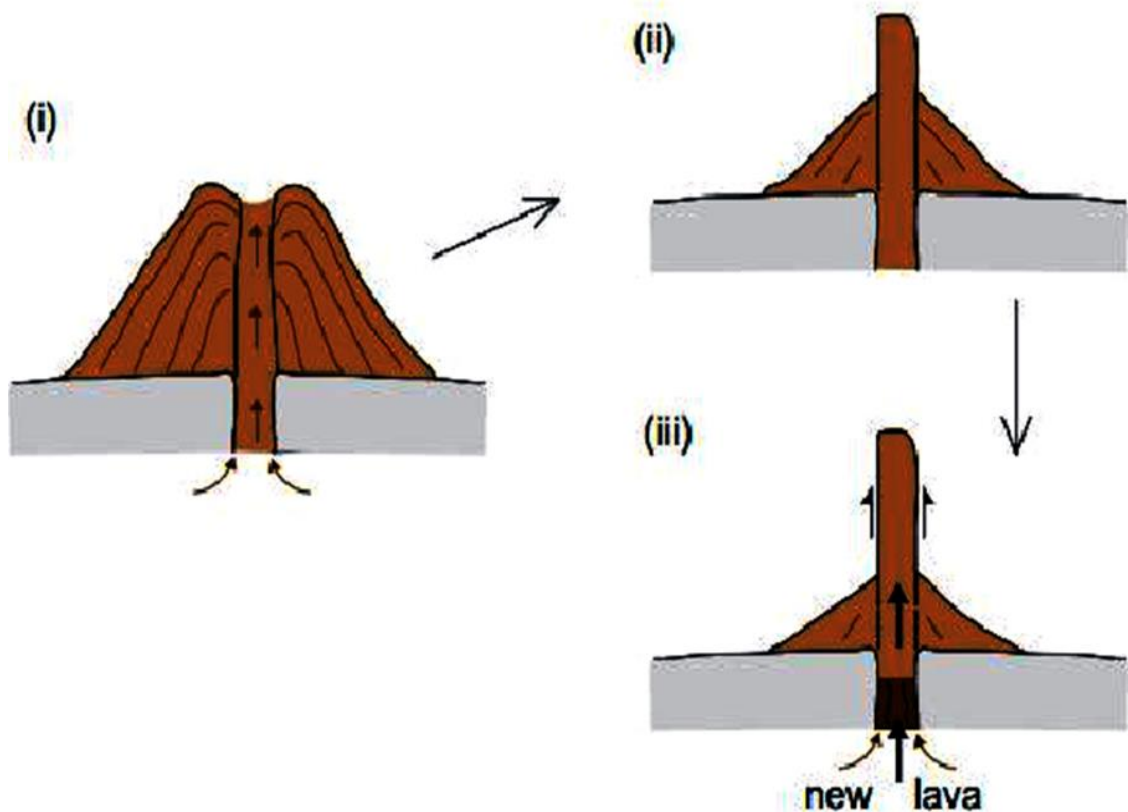


**Figure 2.3** Sketch Illustrating the two possible ways of formation of volcanic plugs of the Adwa area, northern Ethiopia (from Williams, 2016).

- i. Extruded lava forms a steep sided volcanic hill surrounding its vent. When volcanic activity ceases, the whole edifice solidifies.
- ii. Eroded away of the surrounding material, leaving the more resistant one that filled the vent.
- iii. Recommence of volcanic activity; new lava pushes up the material blocking the vent and the plug becomes taller.

Even though there are no radiometric age constraints made on the northwestern Ethiopian volcanic plugs, most researchers (e.g. Daniel Meshesha and Shinjo, 2007; Miruts Hagos et al., 2010) agree that they are of Quaternary age. Volcanic to hypabyssal igneous rocks around Adwa, forming steep-sloped plugs and ridges were produced probably between 7 and 3 Ma (Beyth, 1972). According to Kazmin (1975), the phonolite to trachyte volcanic plugs of Ethiopia are formed probably by tilting and updoming of the sur-

rounding rocks. Natali et al. (2013) have dated the Axum-Adwa basalt and trachyte complex by  $^{40}\text{Ar}/^{39}\text{Ar}$  and K–Ar; 15–19 Ma is recorded as the age of the greater part of the complex, ca. 27 Ma for Trachyte lavas from volcanic centers. The northwestern Ethiopian volcanic plugs, according to Daniel Meshesha and Shinjo, (2007); Dercq et al. (2001) have silica-saturated, alkali-rich trachytic compositions, enriched in incompatible trace elements with negative Sr, Ba, Eu and Ti anomalies. Dercq et al. (2001) have documented that the northern Ethiopian volcanic plugs are feeders of trachytes in shield volcanoes but not to the trap volcanism.

### **2.3. Genesis and Evolution of the Northwestern Ethiopian Volcanic Province**

Representative studies on well exposed northwestern Ethiopian volcanic province, like the Lima Limo and Lalibela sections, to understand the genesis of geochemically distinct basalts (HT2, HT1 and LT suits) and rhyolites, occurred corresponding to those basalts, with the help of trace element, Isotope ratios (Pik et al 1999; Beccaluva et al., 2009;) and helium isotope variations (Marty et al., 1996) confirm that the different suits have different evolutionary histories. The HT2 Oligocene flood basalts exhibit homogeneous compositions, extreme OIB-like REE patterns, relatively higher  $^{87}\text{Sr}/^{86}\text{Sr}$  initial-, lower  $^{143}\text{Nd}/^{144}\text{Nd}$ - and higher  $^{206}\text{Pb}/^{204}\text{Pb}$  -ratios than HT basalts and it suggests the involvement of deep mantle in their genesis whereas, the HT Oligocene flood basalts are characterized by relative depletions in Nb, Ta, Th, and Rb and peaks at Ba and Pb compared to oceanic basalts, depleted lithospheric signature, relatively lower  $^{87}\text{Sr}/^{86}\text{Sr}$  initial-, higher  $^{143}\text{Nd}/^{144}\text{Nd}$ - and lower  $^{206}\text{Pb}/^{204}\text{Pb}$ -ratios than HT2 basalts that implies the involvement of continental crust in their genesis or formed from the melting of a more depleted mantle component (Pik et al., 1998; 1999). Moreover, the genesis of HT2 and LT basalts are well explained by the higher  $^3\text{He}/^4\text{He}$  ratios indicating the contribution of lower-mantle and the lower  $^3\text{He}/^4\text{He}$  ratio suggesting the involvement of crustal materials respectively (Marty et al., 1996). The Afar mantle plume, According to Beccaluva et al. (2009) petrogenetic P-T-X model, is assumed to be thermally and compositionally zoned (Fig. 2.1). This thermally and compositionally zoned mantle plume metasomatizes the mantle at different degrees as its zonation and generates the HT2 basalts and picrites at the hottest and more metasomatized zone and the reverse produces LT basalts. Generally the Ethiopian continental Oligocene flood basalt (both HT and LT) are assumed to be formed as the result of the Afar mantle plume with little contribution from lithospheric mantle (e.g. Furman et

al., 2007; Daniel Meshesha and Shinjo, 2007), though the recent work of Furman et al., (2016) suggests the far more contribution from the metasomatized lithospheric mantle and also explained the formation of HT2 basalts as formed by the drip melting and the HT basalts are originated from shallower, dominantly anhydrous peridotite.

The Oligocene rhyolites of northwestern Ethiopia are formed from the fractional crystallization of associated basalts (Dereje Ayalew et al., 2002; Dereje Ayalew and Gezahegn Yirgu, 2003; Natali et al., 2011); high TiO<sub>2</sub> rhyolites from high TiO<sub>2</sub> basalts and low TiO<sub>2</sub> rhyolites from low TiO<sub>2</sub> basalts whereas, the Miocene-Pliocene Ethiopian volcanic province, mostly shields, are formed by the melting of small compositionally distinct regions (Kieffer et al., 2004). The Quaternary volcanics of northwestern Ethiopian plateau as suggested by Daniel Meshesha and Shinjo, (2007), might have been derived from a more homogenized plume source. Petrogenetic modeling based on rock chemical data and phase equilibria calculations, according to Natali et al. (2013), suggest that the SiO<sub>2</sub>-saturated trachytes and SiO<sub>2</sub>-undersaturated Syenites are generated from the that low-pressure fractional crystallization processes, starting from mildly alkaline- and alkaline basaltic complexes respectively. The relatively similar, with the above justification, evolution of phonolite-trachyte volcanic plugs are explained by Daniel Meshesha and Shinjo, (2007); Miruts Hagos et al. (2010) as the northern and northwestern Ethiopian volcanic plugs are formed by the fractional crystallization of the Miocene- Pliocene (post trap) basalts.

## **CHAPTER THREE**

### **3. METHODOLOGY**

Revision of previous works and related topics, field work, petrography and geochemical analyses are the methods and approaches adopted to achieve the general and specific objectives of this research.

#### **3.1. Revision of Previous Works and Related Topics**

Miruts Hagos et al. (2010) studied the geochemical characteristics of the alkaline basalts and the phonolite–trachyte plugs of the Axum area, northern Ethiopia (Fig 3.1). A geochemical (major and trace element) characteristic of Axum phonolites and trachytes in relation to alkali basalts was their focus. These authors differentiate two magmatic series for the Axum volcanic rocks: The high TiO<sub>2</sub> (2.6–4.4 wt %), Fe<sub>2</sub>O<sub>3</sub> (13.4–17.4 wt %) and high Zr/Nb ratio (9–18) flood basalt sequence, which erupted contemporaneously with the Oligocene Ethiopian flood basalts and the low TiO<sub>2</sub> (2.0–2.6 wt%), Fe<sub>2</sub>O<sub>3</sub> (10.5–14.6 wt%), Zr/Nb ratio (2.8–3.1), and high Nb (60–84 ppm), Th (3.9–7.2 ppm), and Nb/Y ratio (2.2–2.7) post-trap basalt sequence. The values of trace element ratio of phonolite–trachyte plugs are comparable with the trace element ratio of post–trap basalt sequence, the second magmatic sequence, and are indistinguishable from each other. Finally Miruts Hagos et al. (2010) concluded that even though there is the lack of age constraints, from the resemblance of values of trace element ratios of phonolite–trachyte plugs with that of the post–trap basalt sequence, fractional crystallization of post–trap basaltic magmas are responsible for the formation of those volcanic plugs.

Natali et al. (2013) undertook an investigation on the age of Axum-Adwa basalt–trachyte complex (Fig 3.1) and the relationships between basaltic and felsic rocks (Trachytes and Syenites). The Axum-Adwa felsic rocks, as studied by these authors occur as volcanic domes and plugs. The greater part of the complex has an age range 19–15 Ma, whereas trachyte lavas have an age of 27 Ma with <sup>40</sup>Ar/<sup>39</sup>Ar and K–Ar system of age determina-

tion. According to these authors using petrogenetic modeling on geochemical data, trachytes and syenites are formed from the low pressure fractional crystallization of mildly alkaline and alkaline basalts respectively; trachytes are SiO<sub>2</sub> saturated and syenites are SiO<sub>2</sub> undereducated.

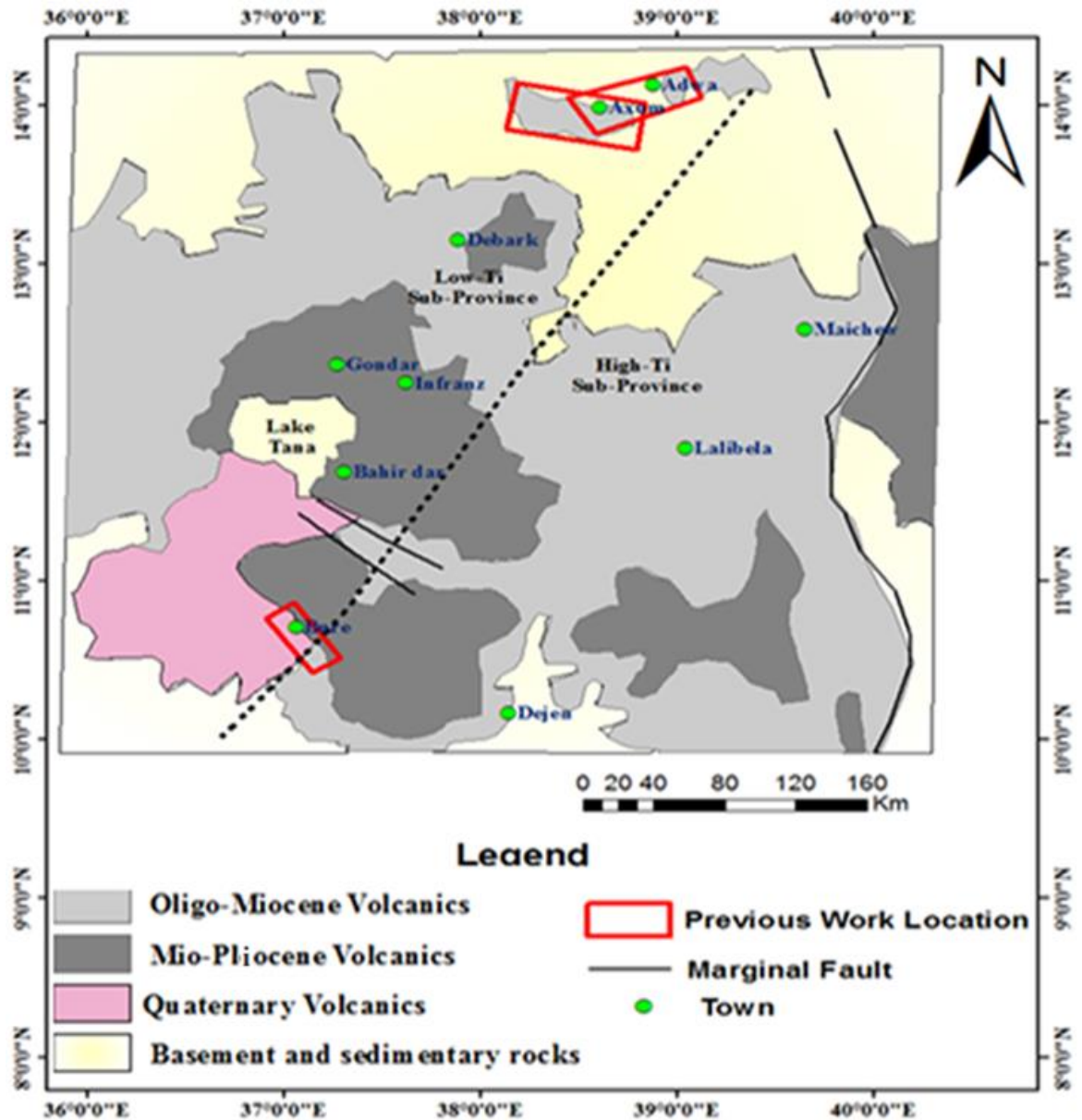


**Figure 3.1** Relative locations of previous studies, rectangular boxes bounded by red lines, related to volcanic plugs (after Miruts et al., 2010). The dashed line shows the proposed boundary between high Ti and low Ti sub-provinces (from Pik et al., 1998).

Another study related to volcanic plugs is conducted by Dercq et al. (2001). These authors consider somehow sparsely distributed volcanic plugs; starting from the volcanic plug located on the Lima Limo section through Gondar- Lake Tana to Debre Tabor. The aim of these authors was to understand the relationships between volcanic plugs of the northwestern Ethiopia and the felsic volcanic rocks of the area. Finally the authors concluded that volcanic plugs of the northwestern Ethiopia are the feeders of trachytes in shield volcanoes but, not for trap volcanics.

From field observation: recent basaltic flows, scoria cones and volcanic plugs of Bure area (Fig 3.1) are emplaced in the Quaternary (Daniel Meshesha and Shinjo, 2007). The trachytes form columnar-jointed upright plugs and the plugs contain coarse- to medium-grained sanidine with trachytic texture. According to TAS and CIPW classification diagrams, the authors pointed out two chemically distinct suites; the hy-qz transitional tholeiitic CFBs and the ne-ol alkaline CFBs, the Quaternary basalts and trachyte plugs.

### **3.2. Field Work**

After the revision of necessary previous works and related topics concerned about volcanic plugs, field work follows. The field work was conducted for a couple of reasons; description of the outcrop and samples, collection of fresh, representative rock samples for thin section and geochemical laboratory analysis, record of GPS locations where samples are taken and take photographs at representative out crop features.

#### **3.2.1. Sampling**

The northern and northwestern Ethiopian plateau consists of volcanics of different age (Fig.3.1); it also contains a number of vertically sided volcanic plugs, the concern of this study. But, the present study volcanic plugs are almost entirely surrounded by Miocene-Pliocene volcanics, particularly the Tarmaber Gussa formation (Fig. 4.1). Volcanic plugs are found in abundance around Infranz. Most of the volcanic plugs of this study are concentrated east of Infranz; except two plugs; one (where sample VP1-NG is taken) around Maksegnt town and the other one (where VP2-SG is taken) around Amed Ber town (Fig 4.1). At each plug, fresh and representative samples were collected.

### **3.3. Petrographic analysis**

Eight samples from eight volcanic plugs have been selected for thin section analysis and prepared in the Geological Survey of Ethiopia, Ethiopia. The petrographic description of each sample and their modal proportion were identified from the prepared thin sections by using petrographic microscope, at the School of Earth Sciences, Addis Ababa University, Addis Ababa Ethiopia.

### **3.4. Geochemical analysis**

A total of eight samples, from eight volcanic plugs were selected from the collected representative samples for major and trace element analysis. The selected samples were sent to the Australian Laboratory Science (ALS), Akaki Kaliti Addis Ababa, Ethiopia for sample preparation. Samples were prepared in the following way: (a) using the crushing instrument (CRU-31 in ALS code) samples were crushed 70 % < 2mm to fine material (b) with the help of riffle splitter (SPL-31 in ALS code), the finely crushed samples were split (c) pulverize split (PUL-31 in ALS code) to 85% < 75 $\mu$ m (d) Crushing control test and pulverizing control test (CRU-QC and PUL-QC in ALS code respectively) were done. After wards, the prepared samples were sent to ALS, Galway, Ireland for major and trace element determinations. The analytical technique Inductively Coupled Plasma Atomic Emission Spectroscopy (ICP-AES) was used to determine the concentration of major elements and base metals. Whole-rock package-ICP-AES (ME-ICP06 in ALS code) and four acid digestions (ME-4ACD81in ALS code) were used to determine the major elements and base metals respectively; total calculations for ME-ICP06 (TOT-ICP06 in ALS code) for major elements is also determined by the instrument ICP-AES. Total volatiles Lost on Ignition (LOI) at 1000°C were determined by WST-SEQ (OAGRA05 in ALS code). Inductively Coupled Plasma Mass Spectrometry (ICP-MS) by lithium borate fusion-ICP-MS (ME-MS81 in ALS code) has been used for the analysis of trace elements.

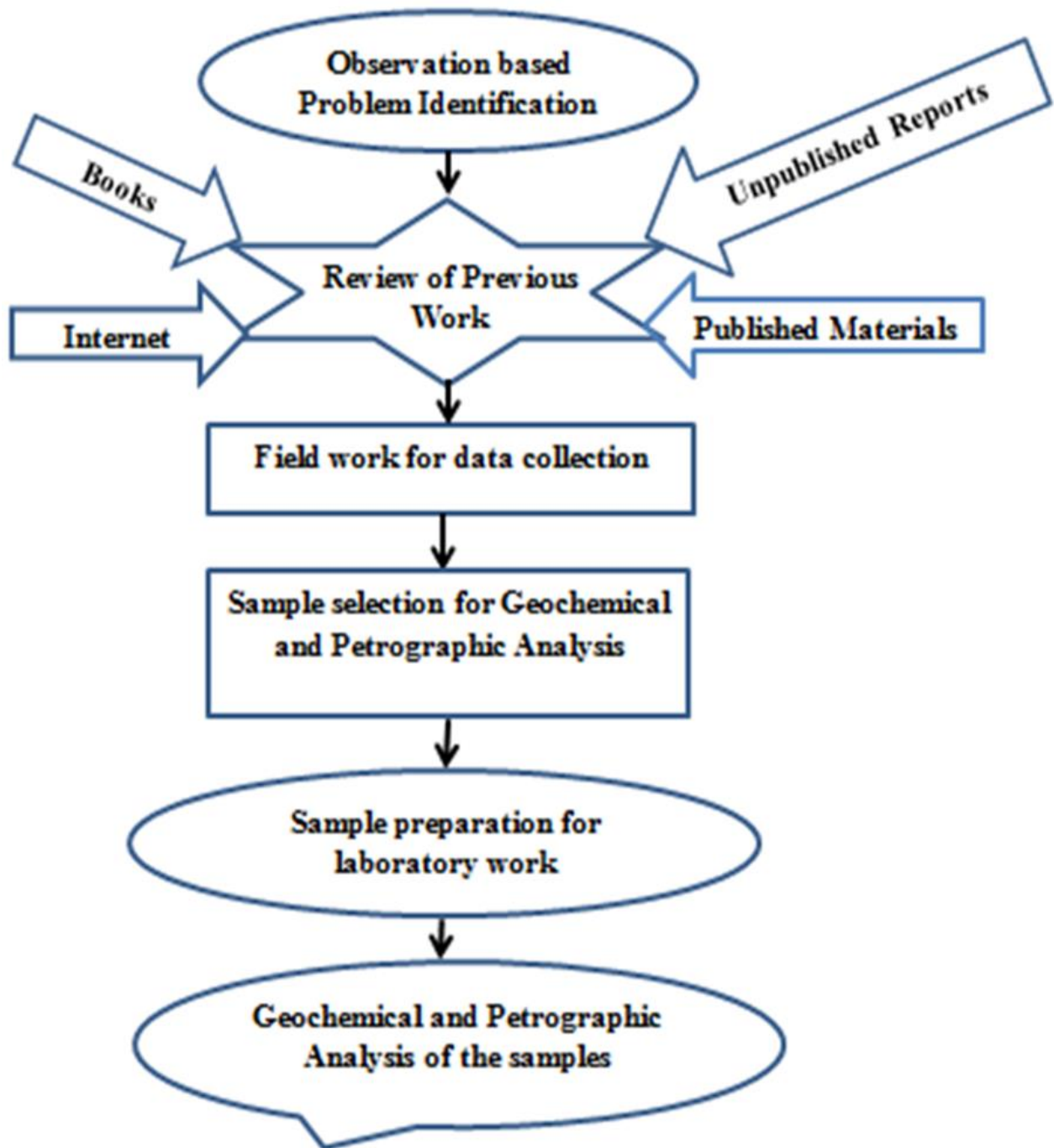


**Figure 3.2** Generalized summary and procedure of the methodology adopted starting from the observation based problem identification to the final geochemical and petrographic analysis of the samples.

## **CHAPTER FOUR**

### **4. FIELD DESCRIPTION AND PETROGRAPHY**

#### **4.1. Field Description**

The northwestern Ethiopian Plateau consists of a number of vertically sided volcanic plugs, the concern of this study. Erosional surfaces of volcanic plugs of the Infranz area, northwestern Ethiopia are almost entirely surrounded by basalts of Tarmaber Gussa formation (Fig. 4.1). The plugs project about an estimated height of 200-300 meters above the present erosional surface of basaltic rocks with 120-200 meters width.

For the purpose of description, the names of volcanic plugs of the study area are according to their local names given by the people living around Infranz, south Gondar zone; samples taken from those plugs (Fig 4.1) are assigned as VP1-NG, VP2-NG, VP3-NG, VP4-NG, VP5-NG, VP6-NG, VP1-SG and VP2-SG to mean volcanic plugs from north and south Gondar, since samples are taken from both north and south Gondar zones. The abbreviation VP implies volcanic plug, the numbers 1, 2, 3... represents the number of volcanic plugs in each zone and this number is given from the northern side to southern side part of the study area in ascending order. The first, six volcanic plugs with the abbreviation NG (to mean north Gondar) after hyphen are from north Gondar and the last, two with the abbreviation SG (to mean south Gondar) are from south Gondar. The description of volcanic plugs is in order of their arrangement from the northern part of the study area to the southern part; sample description taken from each plug is also given in association with the volcanic plug descriptions and the names given for rocks is from the combined field, petrography and geochemical data.

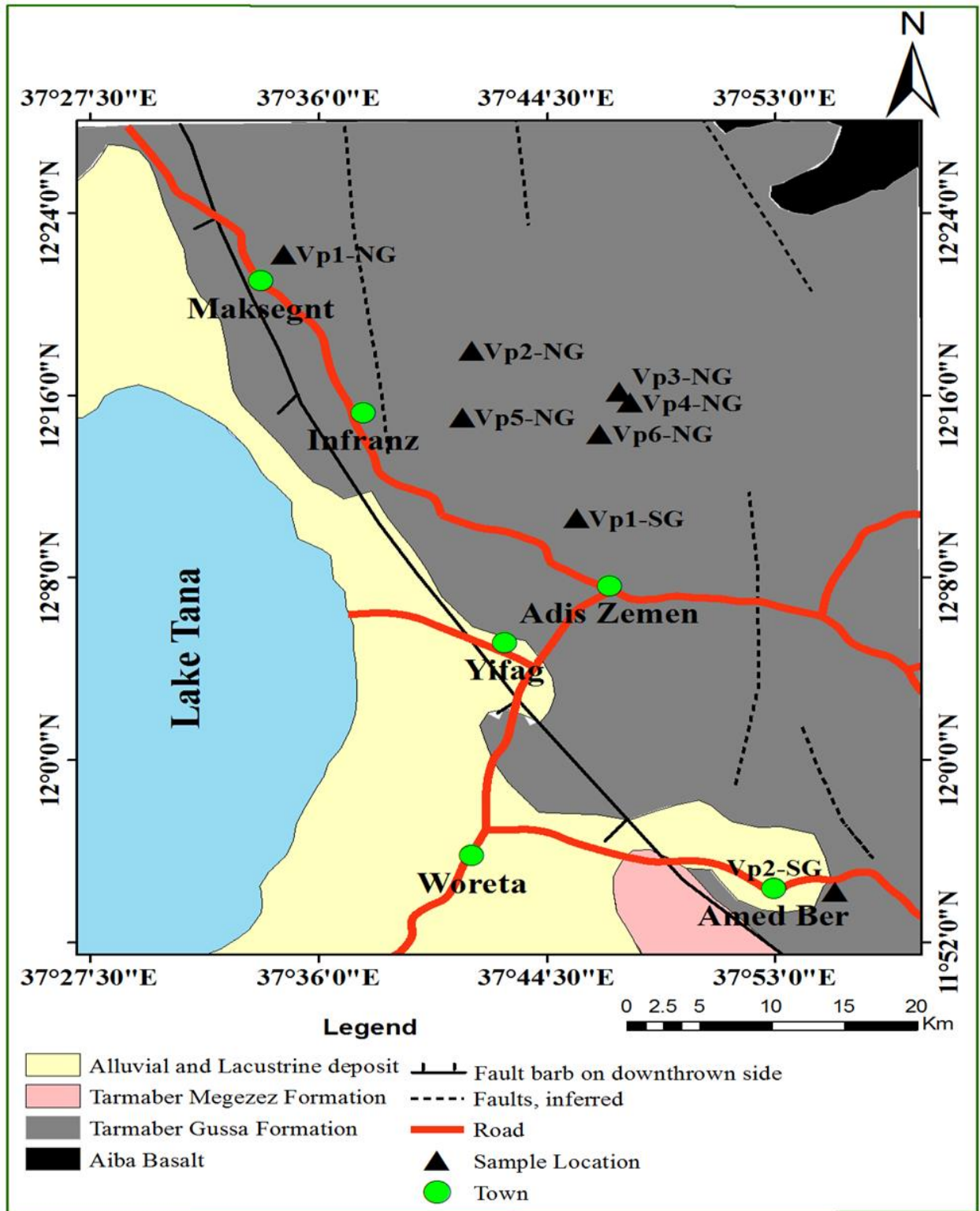


**Figure 4.1** The geological map of the study area, around Infranz, (after Mengesha Tefera et al., 1996) with location and abbreviation of samples taken from volcanic plugs. Since each sample represents one volcanic plug, the location of samples can be considered as the location of volcanic plugs included under this study.

- 1) **Molalit**-This volcanic plug is found at the northern side of the study area and is located around the town, Maksegt. The plug is surrounded by bushes, moderately weathered, characterized by the presence of vertical to sub vertical cracks that reach from the bottom (erosional surface) to the mid and upper part of the volcanic plug (Fig. 4.2A). It ranges from an estimated 200-250m height and 120-150m width. This plug is defined by its fine grained texture; relatively denser in hand specimen samples (VP1-NG) than the other samples taken from other volcanic plugs and is generally dark to light brown weathered and gray fresh color; some dark colored rock fragments are incorporated with this rock. The dark colored rock fragments range in size from coarse to medium grain. The difficult to identify fine grained shiny minerals, probably alkali feldspar, are observed on this volcanic plug.



**Figure 4.2** Field photograph of the volcanic plug, Molalit, found east of Maksegt town; shows vertical to sub vertical cracks that elongate from the bottom, erosional surface, to almost the upper part of the volcanic plug (A). Out crop photograph where sample (VP1-NG) is taken, illustrating the effect of weathering (B).

- 2) **Mender-Mariam**- It is the second (from the northern side of the study area) volcanic plug found north east of Infranz town. This plug makes unique from other volcanic plugs in that it is approximately wide (180-200m) in its diameter with 220-250m height; more or less free of fractures and has massive nature with dark to brown weathered color (Fig 4.3A, B). It is characterized by fine grained; pale colored tra-

chyte rock with very sparsely distribute medium grained shiny minerals probably alkali feldspar. The sample (VP2-NG, Fig 4.1) is taken from this volcanic plug.



**Figure 4.3** (A) Field photograph of the volcanic plug, Mender-Mariam, found north east-east of Infranz; it illustrates the relatively free of fractures which is best seen in (B) that shows the resistance feature of the plug with somehow smooth surface.

**3) Dur-Amba-** This volcanic plug is the third volcanic plug (from the northern side of the study area) and is found somehow east of the town Infranz. The basaltic rock form ridge (horst) surrounding the plug and the plug is found at the graben part which makes it unique from other volcanic plugs. It is the plug with the narrow width (120-140m) with an estimated height of 250-270m. Developed cracks especially horizontal cracks (Fig 4.4B) are observed, also degree of erosional differences between the upper and the more exposed lower part of the plug with brown weathered color. The sample (VP3-NG) is taken from this plug and it is characterized by the fine grained pale colored trachyte rock similar in character with the above two plugs.

**4) Woyni-Amba-** As the first volcanic plug, Molalit, this volcanic plug is also defined by the vertical-to sub-vertical cracks with dark to brown weathered color (Fig 4.5A). It is found east of Infranz town. This plug is relatively wide in diameter (160-180m) than other volcanic plugs but, it is less than Mender- Mariam, and is short in its height (200-220m) with dark weathered color. It shows layering/ banding like the rhyolitic

flow with bell sound when struck with hammer. The sample (VP4-NG, Fig 4.1), is taken from this volcanic plug. This volcanic plug is characterized by the fine grained textured, dark gray fresh colored phonolite with sparsely distributed medium-to-fine-grained shiny minerals probably alkali feldspar and/or feldspathoids.



**Figure 4.4** Field photograph of the volcanic plug, Dur-Amba, found east of Infranz town (A). Out crop photograph of the plug that shows fractures and differences in the degree of weathering between the upper (reddish colored) and lower (pale colored) parts of the plug (B).

**5) Koma-** The fifth volcanic plug (from the northern side of the study area) is called-Koma found east of Infranz and it is the nearest plug for the town Infranz. The area is covered largely by bushes (Fig 4.6A) and the plug shows dark weathered color with an estimated height and width of 240-260m and 150-170m respectively. It is defined by the fine grained, gray fresh colored trachyte with medium-to-fine grained light and brown colored minerals of probably alkali feldspar and biotite. The sample (VP5-NG, Fig 4.1), is taken from this volcanic plug.

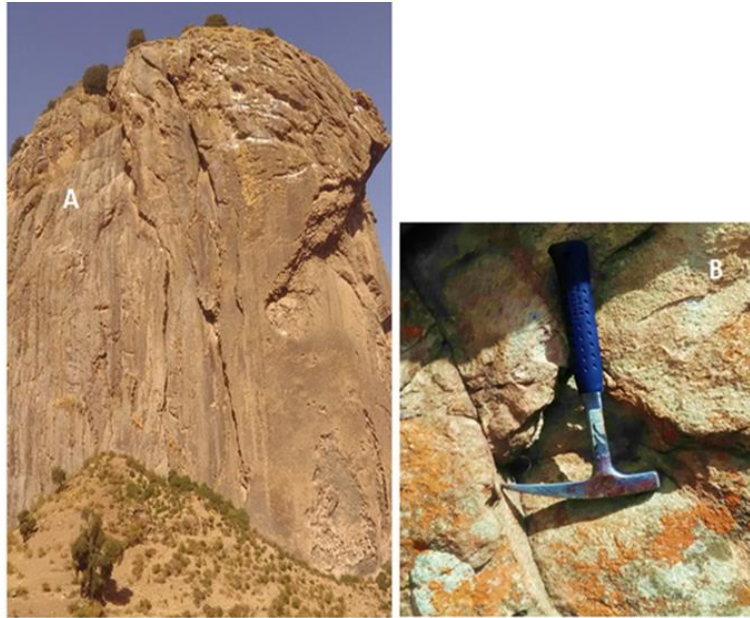


**Figure 4.5** Field photograph of the volcanic plug, Woyni-Amba, found east of Infranz town; shows vertical- to sub- vertical cracks that elongate from the bottom, erosional surface, to almost the upper part of the volcanic plug (A). Out crop photograph of reddish color weathered part of the volcanic plug (B)

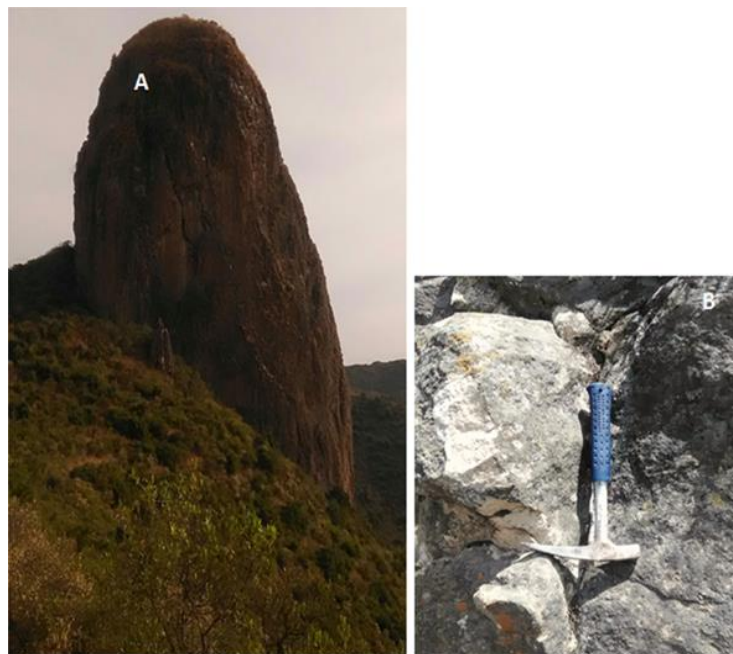


**Figure 4.6** Field photograph of the volcanic plug, Koma, found east of Infranz town. It shows some cracks and surrounded by bushes (A). Out crop photograph of the plug; great boulder like feature is left and the surroundings are eroded away (B).

- 6) **Asiba-** The third volcanic plug (from the southern part of the study area,) and is found again east of the Infranz town is Asiba, with an estimated height and width of 250-270m and 130-150m respectively. Like the plug Mender-Mariam, this plug is almost free of fractures, less weathered with dark brown weathered color. In this plug, as shown in Fig 4.7B, the thin, less resistant, fine grained layer is observed, but is not continuous roundly throughout the plug. Medium- to-fine grained light colored probably alkali feldspar minerals are set in fine grained light gray colored groundmass. The sample (VP6-NG, Fig 4.1), is taken from this volcanic plug.



**Figure 4.7** The less fractured field photograph of the volcanic plug, Asiba, found east of Infranz (A). Out crop photograph that shows the thin, less resistant, but not continuous roundly, layer of the massive volcanic plug (B).

- 7) **Sebaha-** The volcanic plug Sebaha is found north of the town Addis Zemen where the sample VP1-SG is taken (Fig 4.1). This plug is moderately weathered with dark weathered color, 240-260m height and 135-155m width, found on the ridge, in opposite to the volcanic plug Dur-Amba. Moderately weathered nature of this volcanic plug with some fractures is observed in Fig 4.8B. It is fine grained; gray colored trachyte with some medium to fine grained shiny minerals of probably alkali feldspar.
- 8) **Chalmut-** It is the finally sampled volcanic plug during field work and is found at the southern end of the study area, around the town Amed Ber. It has an estimated 250-265m and 135-150m height and width respectively with dark to brown weathered col-

or. This volcanic plug (Fig 4.9A) is grouped under the less weathered and massive volcanic plugs discussed earlier. It is porphyritic textured rhyolite with coarse-to-medium grained quartz crystals set in off-white colored fine grained ground mass. The sample (VP2-SG, Fig 4.1), is taken from this volcanic plug.

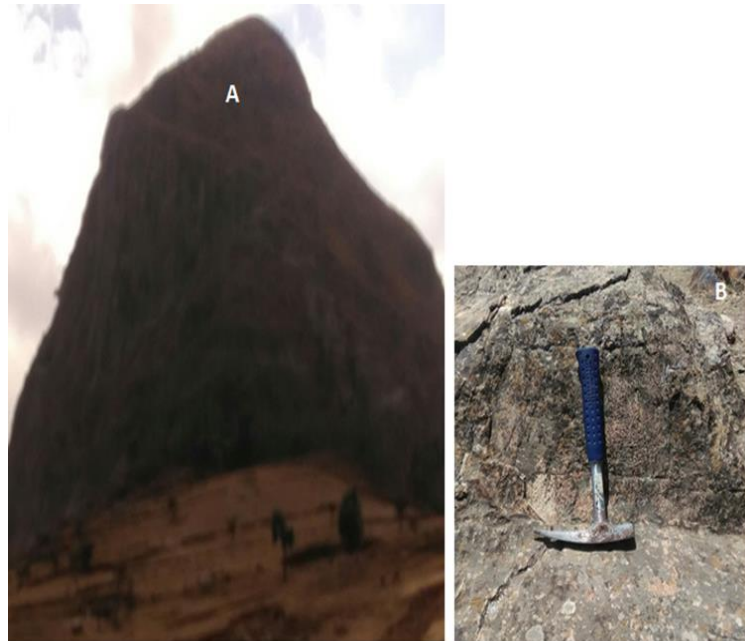


**Figure 4.8** Field photograph of the volcanic plug Sebaha that emplaced on the ridge (A). Out crop photograph of the moderately weathered with some fractures (B).



**Figure 4.9** Field photograph of the volcanic plug, Chalmut, found around Amed Ber; shows the somehow non fractured nature of the plug (A). Out crop photograph of slightly massive and rough surface of the volcanic plug (B).

## **4.2. Petrography**

Eight samples from eight volcanic plugs (one sample from each volcanic plug) were selected for petrographic analysis according to their fresh appearance. The petrographic thin section was prepared in the Geological survey of Ethiopia, Ethiopia. According to Gill (2010) microscopically, rocks can be classified as coarse grained (>3mm), medium grained (1-3mm) and fine grained (<1mm). Therefore here after the petrographic description of samples (scale of grain size) are based on Gill (2010) considerations.

In trachytes continuous flow during the cooling and crystallization of lava produces the alignment of crystals; particularly platy feldspar laths (Philpotts, 2003). These parallel alignments of crystals in most of the samples of volcanic plugs of Infranz area are observed, an indicator of cooling while lava was flowing. The petrographic description of each sample is given below; note that the percentage of phenocrysts and groundmass give in the description is in volume percent. The order of description is the same as the order of the description of volcanic plugs where those samples are taken, the first petrographic sample description is taken from the first and the last from the last volcanic plug described in section 4.1.

- 1) VP1-NG (from Molalit)**-Phenocrysts of large, elongated sanidine, are set in the fine-grained sanidine, albite and opaque to glassy groundmass (Fig. 4.10B). The phenocrysts are elongated, subhedral-to-euhedral, account about 5% and the remaining 95% is the groundmass. The groundmass is composed of thin laths (microlites) to fluidal sanidine (40 %) and albite (30%), fluidal opaque (15%, Fig 4.10A) and glassy matrix (10%). The groundmasses, thin laths of sanidine and albite are settled randomly; hence, it form pilotaxitic texture. It is a pilotaxitic textured sanidine-phyric trachyte.
- 2) VP2-NG (from Mender-Mariam)**-It is composed of micro- phenocrysts of medium-sized, parallelly aligned sanidine (50%) set in the fine grained groundmass containing microlites of sanidine and albite (Fig. 4.11B). The groundmass is composed of microlites of sanidine (~35%) and albite (~15%). A minor amount of opaque minerals with fluidal nature is also observed on the top left corner of Fig 4.11A. The microlites of alkali feldspar and plagioclase on this thin section are parallelly aligned in the same di-

rection as the phenocrysts, indicator of flow while cooling and the rock is sanidine-phyric trachyte with typical trachytic texture.

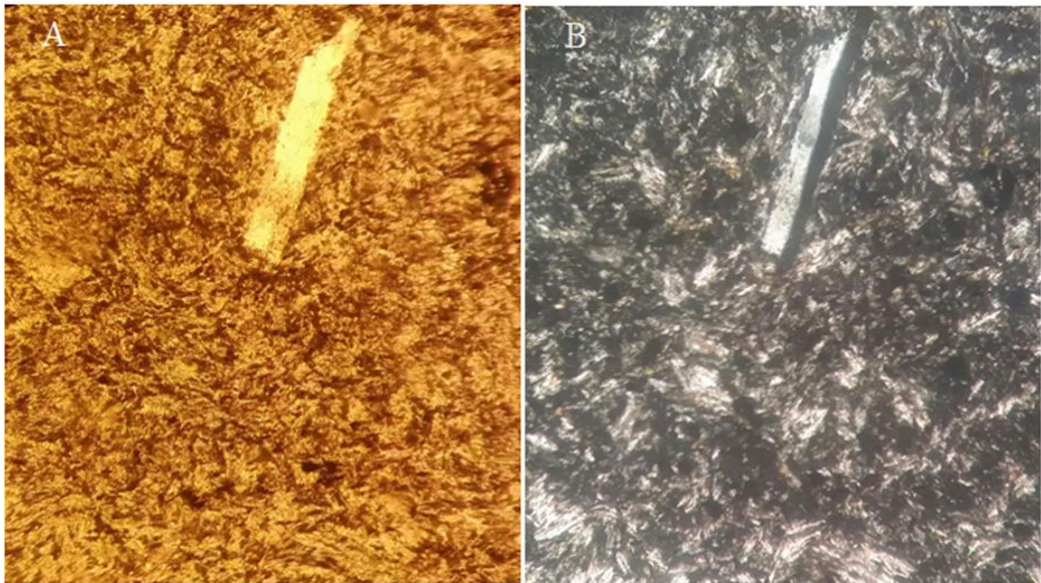


**Figure 4.10** Photomicrographs (VP1-NG) of (A) fluidal dominated nature of opaque groundmass under PPL. (B) The elongated, subhedral-to-euhedral phenocrysts of sanidine under extinction and the fine grained sanidine and sodium plagioclase with some glassy groundmass under XPL. 10X magnification.

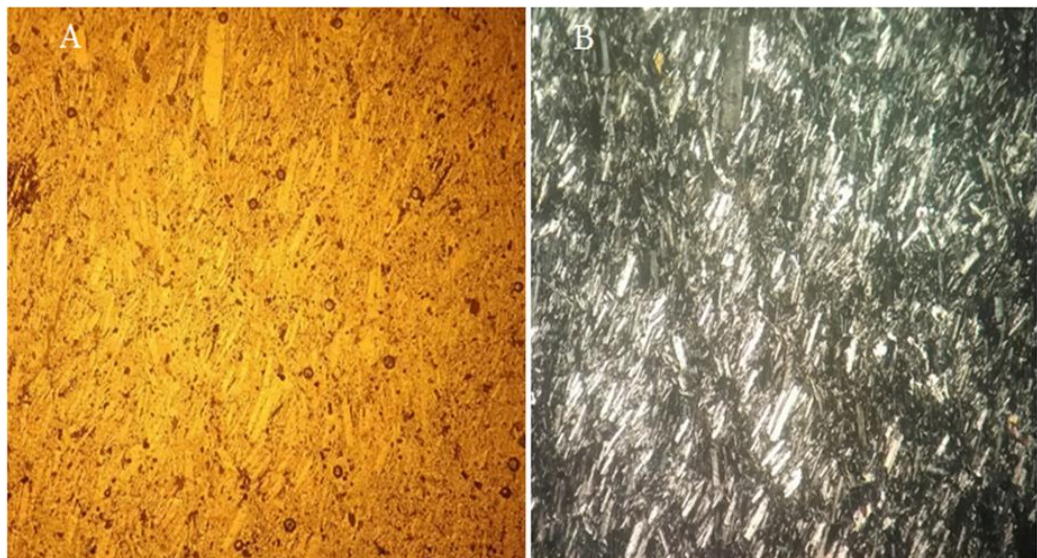


**Figure 4.11** Photomicrographs (VP2-NG) of (A) fluidal nature opaque minerals at the top left corner under PPL. (B) The micro-phenocrysts of sanidine are set in trachytic textured trachyte under XPL. 4X magnification.

- 3) VP3-NG (from Dur-Amba)** - Phenocrysts of medium sized, elongated sanidine (~10-15%) and opaque minerals (~2-3%) are set in the fine grained groundmass. The phenocrysts of sanidine here (Fig 4.12B) are not set parallelly rather randomly. The groundmasses in this thin section are controlled by the fluidal natured opaque minerals (20-23%) which can be better seen in Fig 4.12A, under PPL, sanidine (25-29%) and albite (15-20%). The groundmasses sanidine and albite microlites are parallelly aligned and give the trachytic texture of the rock. The rock is sanidine – phyrlic trachyte.

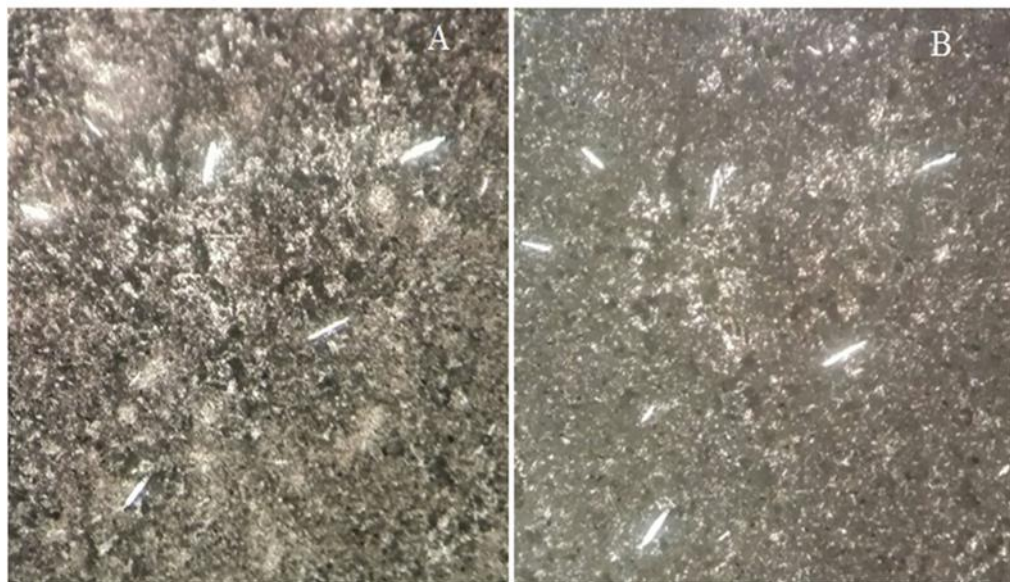


**Figure 4.12** Photomicrographs (VP3-NG) of (A) some, sparsely distributed, phenocrysts and considerable amounts of fluidal opaque PPL. (B) The medium sized randomly oriented phenocrysts of sanidine and some glassy groundmass under XPL. 4X magnification.

- 4) VP4-NG (from Woyni-Amba)**-Is composed of coarse-to-medium sized phenocrysts and micro-phenocrysts set in fine grained to glassy groundmass. The phenocrysts account about 45%; nepheline- (30%), sanidine (13%) and micro-phenocrysts of aegirine-augite (2%). The phenocrysts of nepheline appear as subhedral-to-anhedral and some of them show prismatic nature. The colorless mineral under PPL (Fig 4.13A) found at the center of field of view and dark to light colored with again at the center of field of view under XPL (Fig 4.13B) all are nepheline. The groundmass constitutes about 55%; sanidine accounts about 25%, sodium plagioclase 10%, nepheline (15%), opaque 2% and glass about 3%. The groundmasses of sanidine and sodium plagioclase

class are aligned around the phenocrysts and make trachytic textured nepheline-sanidine- aegirine-phyric phonolite.

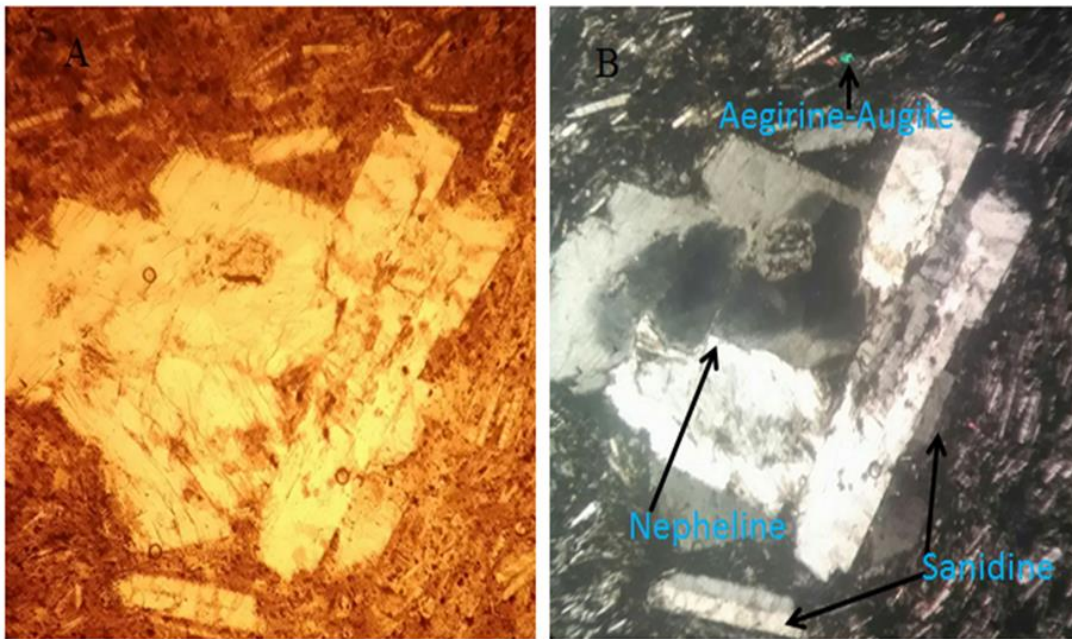


**Figure 4.13** Photomicrographs (VP4-NG) of (A) fluidal nature opaque minerals, especially at the top left corner under PPL. (B) The phenocryst nepheline at the center of field of view and the sanidine with simple twinning; aegirine-augite micro phenocryst is also indicated under XPL.4X magnification.

5) **VP5-NG (from Koma)**- Is composed of phenocrysts of coarse -to -medium size- (~45%) sanidine, biotite and some opaques set in a fine grained sanidine, albite, and opaque groundmass. The phenocrysts are subparallelly-to-randomly oriented, subhedral-to-anhedral sanidine (30%) biotite (~10%) and opaques (~5%). The biotite crystals (Fig 4.14A, B), at the upper left corner, show preferred direction from upper center to upper left corner; some sanidine and opaque crystals exist as inclusions inside the biotite phenocryst. The groundmass constitutes about 55%, of which the sanidine accounts about 33%, albite 15% and opaque 2%. The groundmasses of sanidine and albite are aligned somehow parallelly in the direction biotite crystals are aligned, hence form the trachytic textured, sanidine-biotite-phyric trachyte.

6) **VP6-NG (from Asiba)**- It is composed of phenocrysts of coarse -to -medium sized- (~50%) sanidine and some opaques (e.g. see at the lower left corner of Fig 4.15A) set in a fine grained sanidine, albite, opaque and small proportion of glassy groundmass. Most of the phenocrysts of sanidine are parallelly-to-subparallelly aligned, subhedral-

to-anhedral; phenocrysts constitute sanidine (45%) and opaques (~5%). The groundmass constitutes about 50%, equal volume with that of the phenocrysts of sanidine (32%), albite (15%), opaque (2%) and glass (1%). The groundmasses of sanidine and albite are aligned parallelly forming the trachytic textured, sanidine-phyric trachyte.

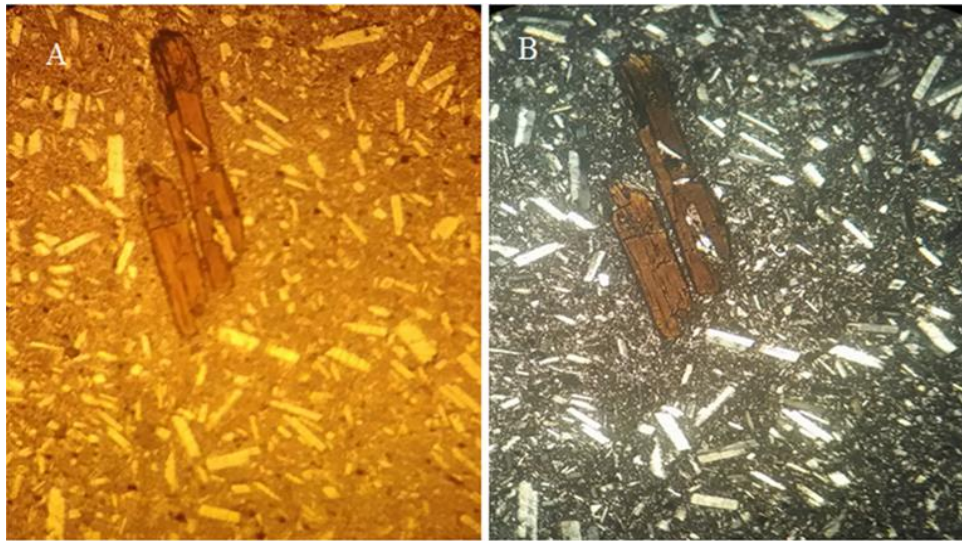


**Figure 4.14** Photomicrographs (VP5-NG) of (A) some opaque phenocrysts and two parallelly aligned biotite crystals under PPL. (B) The phenocrysts of sanidine under extinction and the fine grained sanidine and albite groundmass under XPL. 4X magnification.

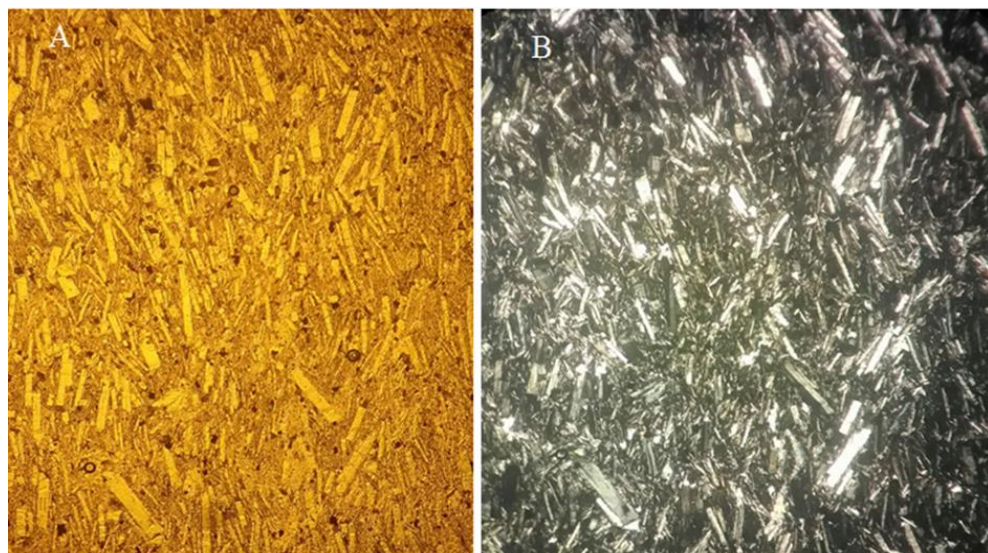


**Figure 4.15** Photomicrographs (VP6-NG) of (A) small phenocrysts, micro phenocrysts and groundmass of opaque minerals, under PPL. (B) The subparallelly-to-parallelly aligned phenocrysts of sanidine, some of them are under extinction and the fine grained alkali feldspar groundmass; small proportion of glassy groundmass is also evident. 4X magnification.

- 7) VP1-SG (from Sebaha)-** Is composed of phenocrysts of coarse -to -medium sized - (~35%) sanidine and small anhedral opaques set in a fine grained groundmass. The phenocrysts of sanidine which accounts about (30%) are parallelly-to-subparallelly aligned, subhedral-to-anhedral and opaques are anhedral with an estimated volume of (~5%).The groundmass is composed of alkali feldspar, particularly sanidine, albite, opaques and small proportion of glass. The groundmass constitutes about 65%, which is more than that of the proportion of phenocrysts; an estimated volume percentage for the groundmass is of sanidine (38%), albite (20%), fluidal opaque (5%), and glass (2%). The microlites or very fine grained groundmasses of sanidine and albite are parallelly aligned, so that it forms trachytic textured sanidine -phyric trachyte rock.
- 8) VP2-SG (from Chalmut) -**It is composed of phenocrysts of large -to –medium sized quartz, large sized sanidine, elongated biotite and opaque minerals set in almost glassy groundmass. Phenocrysts are characterized by the subhedral-to-euhedral shape; micro-phenocrysts of quartz and probably pyroxene are also observed. Phenocrysts account about 52 %; quartz (25%), sanidine (22%), biotite (3%) and opaque (2%). The groundmass constitutes about 48%; glass (30%), microlites of sanidine (9%), quartz (7%) and opaque (2%). sanidine microlites show slight parallel to subparallel orientation that form trachytic textured quartz-sanidine-biotite phyric rhyolite.

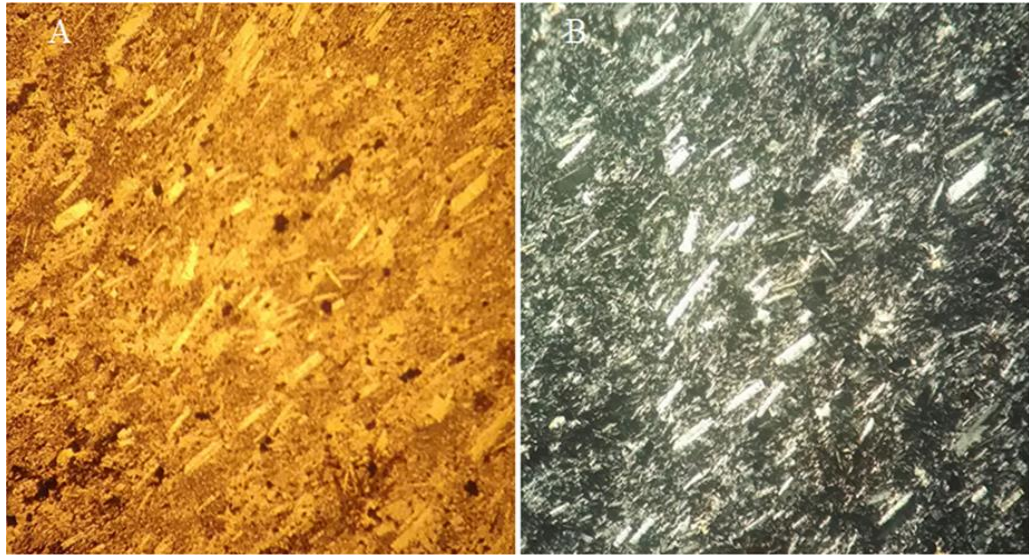


**Figure 4.16** Photomicrographs (VP1-SG) of (A) fluidal opaque groundmass especially observed at the bottom left corner and anhedral phenocrysts under PPL. (B) The parallel aligned phenocrysts of alkali feldspar particularly sanidine, partly under extinction and the fine grained alkali feldspar groundmass under XPL.4X magnification.

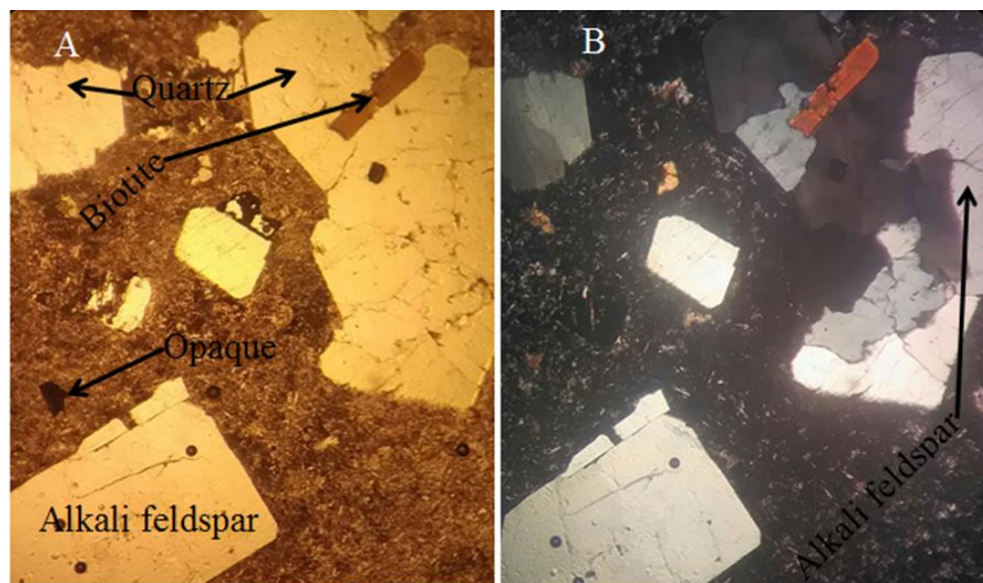


**Figure 4.17** Photomicrographs (VP2-SG) of (A) subhedral-to-euhedral opaque phenocrysts and fluidal nature opaque groundmass under PPL. (B) Phenocrysts of dominantly quartz, some of them are under extinction and alkali feldspar under XPL. 4X magnification.

## **CHAPTER FIVE**

### **5. RESULT OF GEOCHEMICAL ANALYSIS**

#### **5.1. Major Elements**

The data of major elements determined by Inductively Coupled Plasma Atomic Emission Spectroscopy (ICP-AES) and trace elements by Inductively Coupled Plasma Mass Spectrometry (ICP-MS) for the representative samples of volcanic plugs from Infranz area are presented in table 5.1. The plots of major element oxides in all the preceding diagrams are anhydrous normalized.

Samples from volcanic pugs of the Infranz area, northwestern Ethiopia, Table 5.1, show concentrations of SiO<sub>2</sub> between 59.6 and 75.4 wt. %, but most of them are clustered around 66 wt. %; TiO<sub>2</sub> less than 0.5 wt. %, except two samples, VP1-NG, 0.73 and VP4-NG, with 0.54 wt. %; Al<sub>2</sub>O<sub>3</sub> varies between 13.9-19.2 wt. %. The MgO and CaO concentrations for the majority of the samples are less than 0.34 and 0.76 wt. % respectively, however VP1-NG (MgO=1.22, CaO= 2.01 wt. %), VP4-NG (CaO=1.19 wt. %) have relatively higher values. Na<sub>2</sub>O wt. % is greater than K<sub>2</sub>O wt. % in all the samples; there are no any significant differences on other major element oxide concentrations.

The Lima Limo rhyolites taken from Dereje Ayalew and Gezahegn Yirgu (2003) of (see appendix one) selected to understand the feeding nature of volcanic plugs for the surrounding volcanic rocks, ranges in SiO<sub>2</sub> concentration approximately from 60 to 76 wt. %. The difference in the concentration of samples from volcanic plugs (This study) and the Lima Limo rhyolites is that: Al<sub>2</sub>O<sub>3</sub> content is higher in the samples of volcanic plugs 13.9-19.2 wt. % than rhyolites 11.8-15 wt. %. In terms of Na<sub>2</sub>O and K<sub>2</sub>O wt. % concentrations, there is a great difference; Na<sub>2</sub>O is higher in all the samples of volcanic plugs (Na<sub>2</sub>O>K<sub>2</sub>O), whereas the later shows more K<sub>2</sub>O is higher in all the samples of the Lima Limo rhyolites (K<sub>2</sub>O>Na<sub>2</sub>O). Otherwise there are no significant variations in the concentration of major elements between Infranz volcanic plugs and Lima Limo rhyolites.

**Table 5.1** Major and trace element geochemical analysis result of representative rock samples from volcanic plugs of the Infranz area, northwestern Ethiopia.

<b>Sample:</b>	<b>VP4-NG</b>	<b>VP1-NG</b>	<b>VP2-NG</b>	<b>VP3-NG</b>	<b>VP6-NG</b>	<b>VP5-NG</b>	<b>VP1-SG</b>	<b>VP2-SG</b>
Rock type:	Phonolite	Trachyte	Trachyte	Trachyte	Trachyte	Trachyte	Trachyte	Rhyolite
Lat. E:	12°15'39"	12°22'10"	12°17'56"	12°16'08"	12°15'01"	12°15'39"	12°10'35"	11°54'12"
Long. N:	37°47'12"	37°34'42"	37°41'42"	37°47'12"	37°46'28"	37°41'21"	37°45'36"	37°55'13"
SiO <sub>2</sub>	59.6	61.2	66.2	66.4	66.5	66.6	66.9	75.4
TiO <sub>2</sub>	0.54	0.73	0.28	0.36	0.3	0.3	0.27	0.26
Al <sub>2</sub> O <sub>3</sub>	19.2	16.85	16.85	16.85	17.25	17.05	16.5	13.9
Fe <sub>2</sub> O <sub>3t</sub>	3.14	5.33	3.5	3.19	3.65	3.46	3.41	1.29
MnO	0.32	0.49	0.25	0.37	0.26	0.21	0.3	0.02
MgO	0.33	1.22	0.34	0.31	0.23	0.15	0.15	0.15
CaO	1.19	2.01	0.76	0.54	0.52	0.44	0.51	0.23
Na <sub>2</sub> O	8.45	6.66	6.66	7.48	6.59	6.71	6.68	4.89
K <sub>2</sub> O	6.09	4.99	5.63	5.71	5.6	5.66	5.69	4.99
P <sub>2</sub> O <sub>5</sub>	0.09	0.15	0.13	0.11	0.12	0.1	0.12	0.06
LOI	1.36	1.64	0.43	0.4	0.89	0.75	0.49	0.71
Total	100.31	101.27	101.03	101.72	101.91	101.43	101.02	101.9
CIPW Norm								
Q			4.98	2.05	5.74	5.45	5.97	26.99
C								0.18
Or	36.37	29.60	33.07	33.30	32.76	33.22	33.33	29.14
Ab	37.23	55.68	54.99	54.16	55.20	55.81	54.51	40.89
An		1.35			0.94			0.74
Ne	15.34	0.48						
Di	1.80	5.50	1.82	1.51	0.64	0.80	0.80	
Hy				0.06	0.27			0.37
Ol		0.35						
Mt			0.00	0.16			0.19	
Il	0.69	1.05	0.53	0.67	0.55	0.45	0.51	0.04
Ap	0.21	0.35	0.30	0.25	0.28	0.23	0.28	0.14
Ac	5.92		0.90	7.32		0.52	1.34	
Wo	1.02		0.24			0.11	0.29	
Hm	1.13	5.35	3.16	0.51	3.61	3.26	2.78	1.27
Tn					0.02	0.15		
Ru								0.23

Pf	0.31	0.30						
Li	20	30	20	20	20	20	20	20
Sc	1	10	5	4	8	8	7	1
V	11	60	<5	5	5	6	<5	9
Cr	10	30	10	20	10	10	10	10
Co	<1	9	1	<1	1	<1	<1	<1
Ni	3	5	24	2	1	<1	1	2
Cu	<1	8	1	<1	<1	<1	<1	<1
Zn	142	244	131	173	125	116	132	20
Ga	29.4	31.8	24.8	30.1	23.4	23.7	22.2	21.6
As	8	5	5	<5	<5	<5	<5	5
Rb	161	137.5	111.5	150	112.5	116.5	135.5	175
Sr	139	157	21.4	3.3	17.4	11.4	11.6	127.5
Y	50.4	43.5	46.3	50.9	42.5	39.4	40.4	31.9
Zr	989	986	750	1250	852	912	826	314
Nb	259	270	182.5	285	204	224	202	135
Mo	20	4	3	<1	3	3	4	3
Ag	<0.5	0.6	0.5	0.5	<0.5	<0.5	<0.5	<0.5
Cd	<0.5	<0.5	<0.5	<0.5	<0.5	<0.5	<0.5	<0.5
Sn	3	4	3	5	3	4	3	4
Cs	2	0.91	0.24	0.52	0.16	0.34	0.42	0.84
Ba	300	110	248	19.8	196	117	134.5	185
La	187	103	126	156	120	108	117	57.9
Ce	329	177.5	232	295	208	190	210	133.5
Pr	30.3	16.35	22.7	28.6	19.4	20.7	20.9	10.7
Nd	103	55	82.3	101	73.8	69.7	75.5	35.3
Sm	14.4	8.92	13.5	15.7	11.2	11.25	12.3	5.74
Eu	2.83	2.08	2.32	2.47	2.11	2.08	1.9	0.63
Gd	9.04	6.53	8.68	8.95	7.58	7.58	8.26	3.57
Tb	1.59	1.18	1.41	1.6	1.35	1.14	1.27	0.74
Dy	8.48	7.13	8.48	9.11	7.47	7.28	7.86	4.38
Ho	1.61	1.51	1.6	1.78	1.51	1.51	1.52	1.03
Er	5.38	4.43	4.48	5.57	4.71	4.46	5.02	3.52
Tm	0.84	0.86	0.77	0.85	0.75	0.67	0.73	0.59
Yb	5.82	5.82	5.85	6.57	5.23	5.56	5.53	4.35
Lu	0.89	0.89	0.97	0.9	0.85	0.89	0.85	0.67
Hf	19.2	21.4	16.5	25.3	17.6	19.6	17.5	10.8
Ta	15.7	16.1	10.7	17	11.8	13.7	12.2	10.2

---

W	2	2	1	1	2	1	3	3
Tl	<10	<10	<10	<10	<10	<10	<10	<10
Pb	3	13	9	23	2	<2	4	5
Th	26.7	25.3	18.85	28.7	19.95	21.4	20.5	26.9
U	8.49	702	4.48	6.93	4.29	4.44	5.19	5.73

Major elements including LOI and CIPW norm in weight percent (wt. %), trace elements in parts per million (ppm), LOI= total volatiles lost on ignition, total Fe as Fe<sub>2</sub>O<sub>3</sub>. CIPW norm calculations are from spreadsheet (Lowenstern, 2000) with Fe<sup>2+</sup>/Fe<sup>3+</sup> ratio=1:1.

On the total alkali versus silica (Les Bas et al., 1986) classification diagram (Fig.5.1), most samples of the volcanic plugs plot in the field of trachyte. Of the eight samples of volcanic plugs, two plot in the other fields: one in the phonolite and the other in the rhyolite; the entire samples plot in the alkaline region, except one sample (VP2-SG) which plots in the transitional region. Most samples of the volcanic plugs are quartz normative (table 5.1), which ranges between approximately from 2-27 wt. %, except two samples (VP1-NG and VP4-NG) which rather are nepheline normative. Most of the samples contain normative acmite and so, they are peralkaline. All the samples of previously studied, Lima Limo rhyolites, plot in the subalkaline region and are dominated by the rhyolitic composition with the exception of two samples, one in the trachy-andesite and the other in the trachyte fields.

The variation diagrams of major element oxides versus silica are plotted in Fig. 5.2. It is difficult to say there are strict negative, positive or inflated trends that could be solely explained by fractional crystallization between Infranz volcanic plugs themselves and with that of the Lima Limo rhyolites. But, somewhat weak trends are observed between the Infranz volcanic plugs and again between Lima Limo rhyolites. To express the trends in relative terms: MgO, MnO, TiO<sub>2</sub> and P<sub>2</sub>O<sub>5</sub> versus SiO<sub>2</sub> wt. % plots highlight the presence of negative trends of the Infranz volcanic plugs and Lima Limo rhyolites, especially the earlier one. Fe<sub>2</sub>O<sub>3</sub>t, Al<sub>2</sub>O<sub>3</sub> and CaO versus SiO<sub>2</sub> wt. % plots illustrate the presence of distinct trends, all negative, between the Infranz volcanic plugs and the Lima Limo rhyolites whereas, K<sub>2</sub>O versus SiO<sub>2</sub> wt. % variation diagram tend to show distinct-

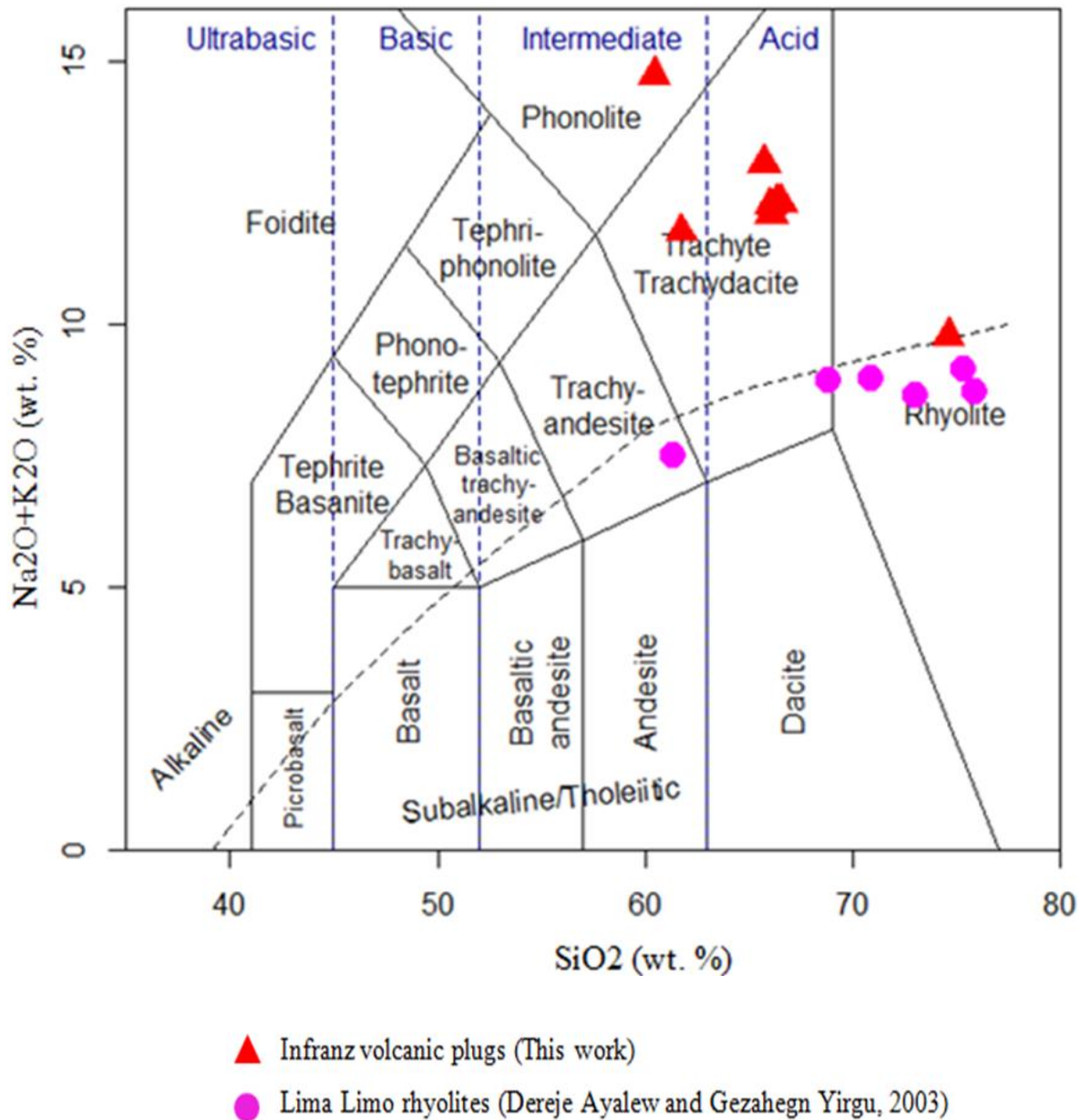
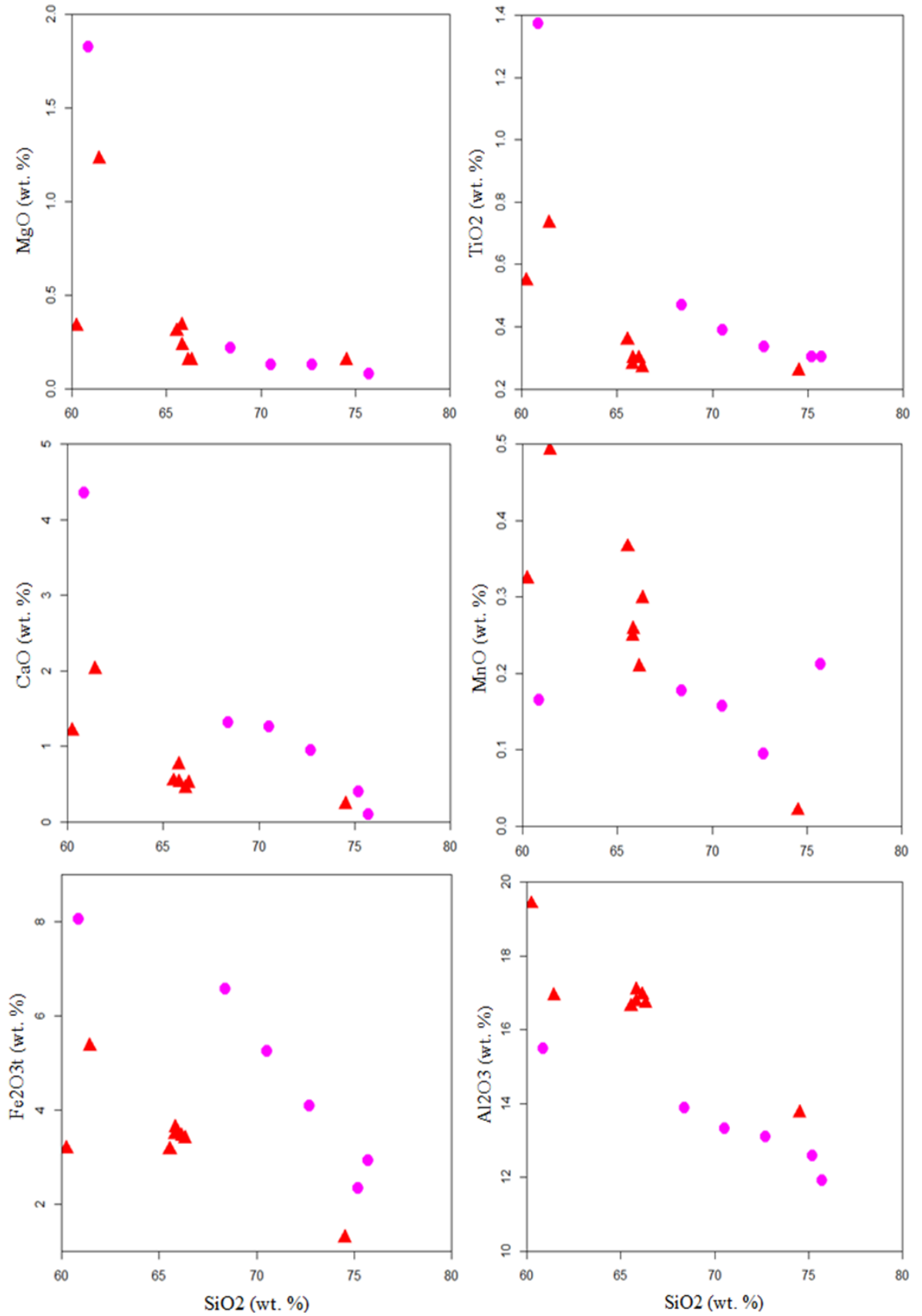


**Figure 5.1** A plot of total alkali ( $\text{Na}_2\text{O}+\text{K}_2\text{O}$  wt. %), versus silica ( $\text{SiO}_2$  wt. %), (Les Bas et al., 1986) for samples of volcanic plugs from Infranz area and volcanic rocks from Lima Limo area; with data for Lima Limo volcanic rocks from Dereje Ayalew and Gezahegn Yirgu (2003).

opposite, negative for Infranz volcanic plugs and positive for the Lima Limo rhyolites, trends. The  $\text{Na}_2\text{O}$  versus  $\text{SiO}_2$  wt. % variation diagram clearly illustrate the negative trends between Infranz volcanic plugs and no trend between the Lima Limo rhyolites. In most of the major element oxide variation diagrams, the sample VP2-SG (rhyolitic in composition) goes along with the samples from Lima Limo rhyolites.

In the MnO versus SiO<sub>2</sub> wt. % variation diagram, most of the Infranz volcanic plugs tend to show higher values of MnO at a given value of SiO<sub>2</sub> but, one sample from the volcanic plugs show the lowest MnO content than all the Lima Limo rhyolites. Similarly, in the variation diagrams of Al<sub>2</sub>O<sub>3</sub> and Na<sub>2</sub>O versus SiO<sub>2</sub> wt. %, most of the Infranz volcanic plugs show higher concentration of Al<sub>2</sub>O<sub>3</sub> and Na<sub>2</sub>O at a given SiO<sub>2</sub> content. On the contrary, Infranz volcanic plugs tend to show lower concentrations of TiO<sub>2</sub>, Fe<sub>2</sub>O<sub>3t</sub> and CaO in TiO<sub>2</sub>, Fe<sub>2</sub>O<sub>3t</sub> and CaO versus SiO<sub>2</sub> wt. % variation diagrams. Unlike the other variation diagrams, there is no/little clear concentration variation in K<sub>2</sub>O, MgO and P<sub>2</sub>O<sub>5</sub> versus SiO<sub>2</sub> variation diagrams between the Infranz volcanic plugs and the Lima Limo rhyolites.

One distinct feature of most of the compositionally trachyte volcanic plugs of the Infranz area is that they cluster around the same SiO<sub>2</sub> and other major element oxide concentrations in most of the major element variation diagrams; this may suggest the little effect of fractional crystallization, between them, in their formation, This clustering of samples around the same SiO<sub>2</sub> and other major oxide concentrations exclude the samples from three volcanic plugs; two samples of normative quartz free phonolitic VP4-NG and trachytic VP1-NG and one sample which is not only by normative, but also by modal quartz rich-rhyolitic VP2-SG.



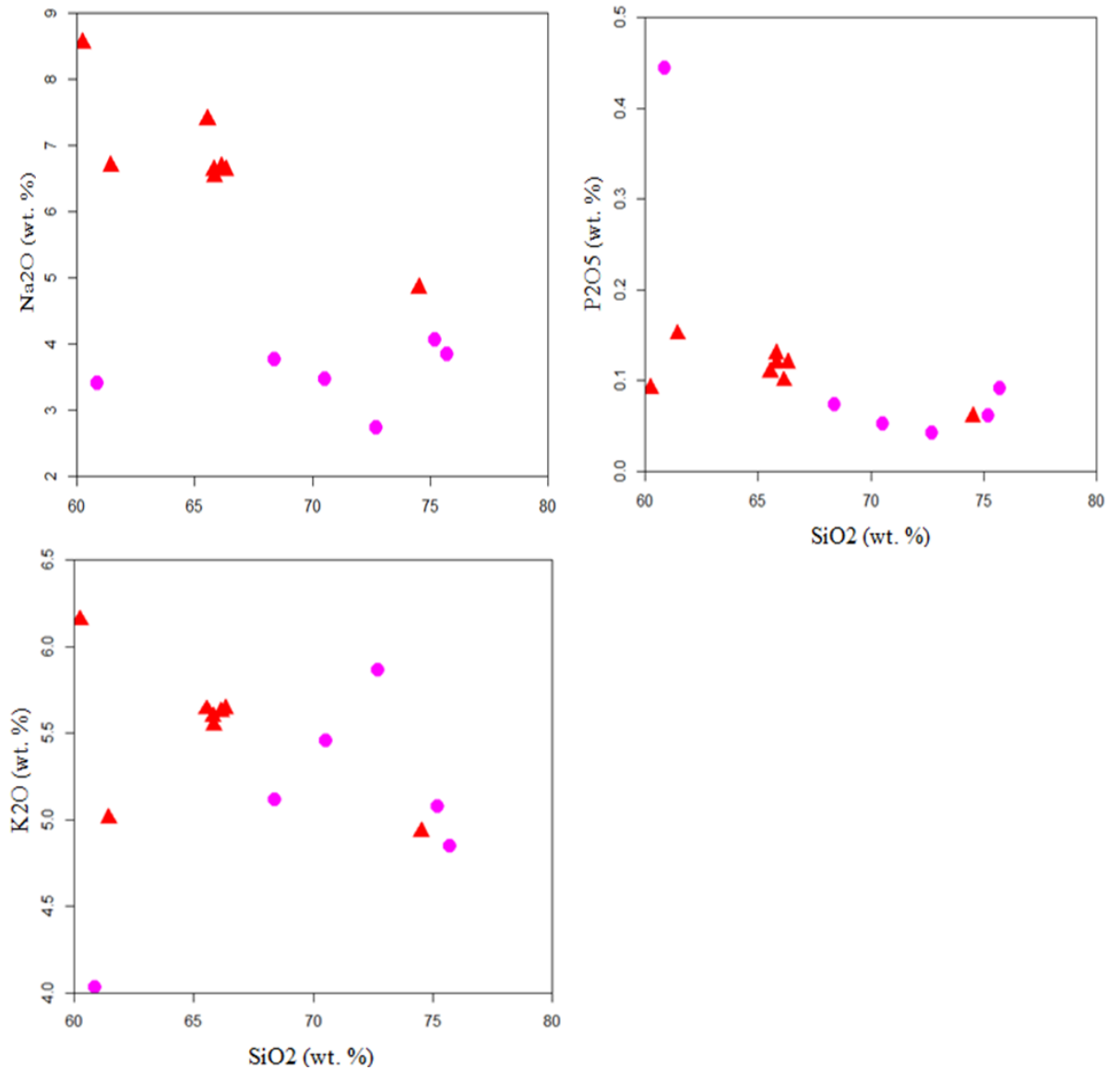


**Figure 5.2** Variation of the major element oxides versus SiO<sub>2</sub> (wt. %) for the Infranz volcanic plugs and Lima Limo rhyolites. Data source for Lima Limo rhyolites and symbols are as in Fig. 5.1.

The distinct trends Lima Limo rhyolites form and rather similar concentrations Infranz volcanic plugs show in most of the major element oxides versus silica variation diagrams may be due to source heterogeneity.

## **5.2. Trace elements**

Selected incompatible trace elements versus silica variation diagrams (Fig.5.3) reveal that the Infranz volcanic plugs form from slightly negative trends to dispersed ones (no trend). The Nb and Yb ppm versus SiO<sub>2</sub> wt. % diagrams between volcanic plugs show a little bit negative trend, correlates with SiO<sub>2</sub> negatively, whereas trends are not observed on the other variation diagrams, rather they illustrate almost similar concentrations of incompatible elements at a given SiO<sub>2</sub> content. Ba ppm versus SiO<sub>2</sub> wt. % plot for Infranz volcanic plugs and Lima Limo rhyolites show slight trend but, all other variation diagrams do not form any trend.

Like that of most major element oxides do in most of the Infranz volcanic plugs, especially trachytic ones, show limited rang in the concentration of trace elements in the variation diagrams of trace elements versus silica (Fig 5.3). Trace element concentrations between the Infranz volcanic plugs and the Lima Limo rhyolites ranges from highly variable in Nb, Th and Yb, slightly variable in Ba to almost similar in Zr and Rb. In the variation diagrams of Nb, Th and slightly Ba ppm versus SiO<sub>2</sub> wt. %, the Infranz volcanic plugs tend to show higher concentrations of Nb, Th and Ba than the Lima Limo rhyolites at a given SiO<sub>2</sub> content. On the contrary, in the Yb ppm versus SiO<sub>2</sub> wt. % variation diagrams, Infranz volcanic plugs tend to show lower Yb concentration than the Lima Limo rhyolites. In the Zr and Rb ppm versus SiO<sub>2</sub> wt % variation diagrams, almost similar concentrations of Zr and Rb at a given SiO<sub>2</sub> concentrations are observed between Infranz volcanic plugs and Lima Limo rhyolites.

The almost similar concentrations of trace elements, as major element oxides do, between Infranz volcanic plugs and the slightly negative to no trends trace elements form with silica may suggest the little effect of fractional crystallization between those volcanic plugs in their formation. The noticeable variations in the concentrations of trace elements between the Infranz volcanic plugs and the Lima Limo rhyolites may suggest the source heterogeneity.

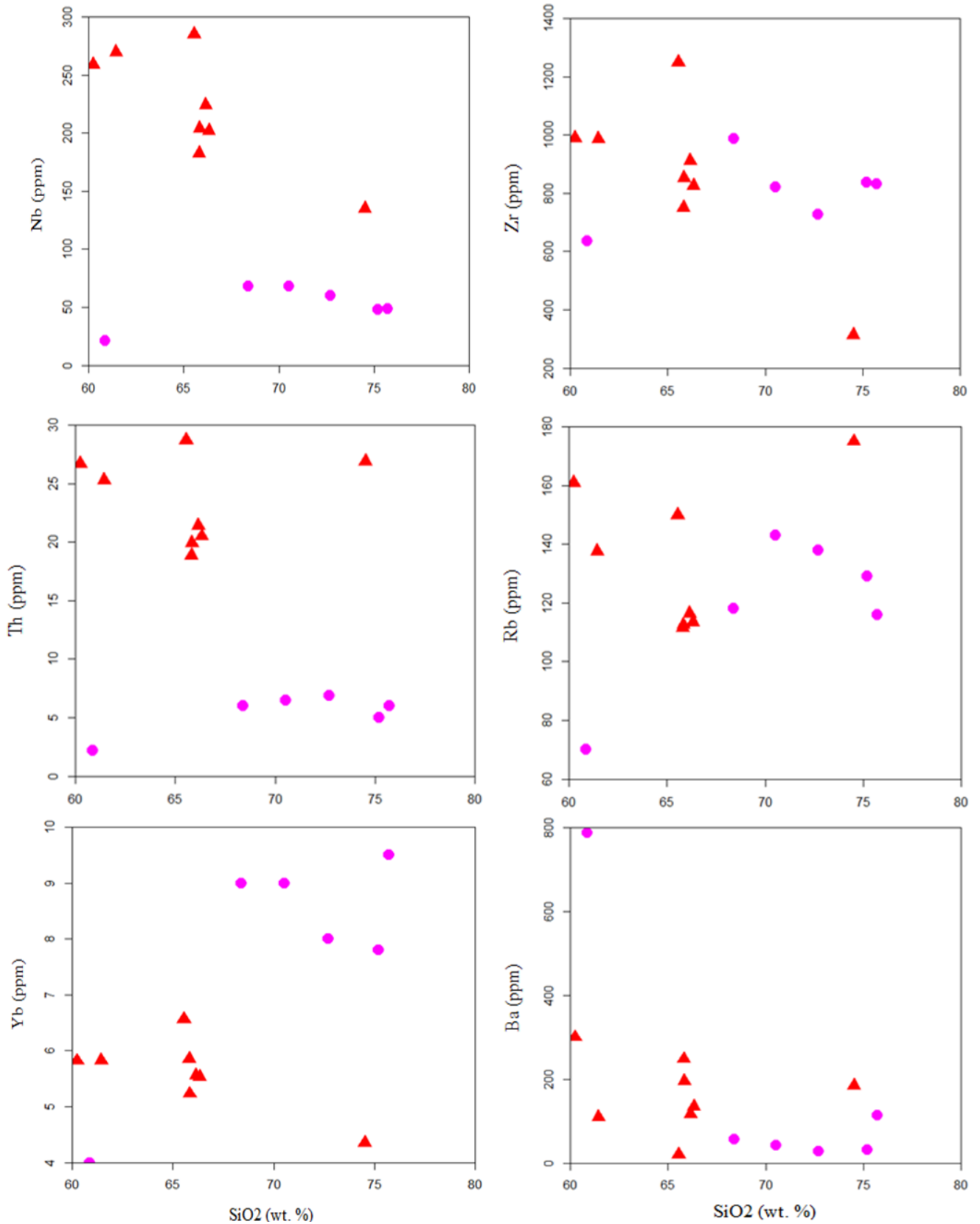


**Figure 5.3** Selected incompatible trace elements (ppm) versus silica (wt. %) variation diagrams. Data source for Lima Limo rhyolites and symbols are as in Fig. 5.1.

The most incompatible trace element-element and trace element ratio- ratio variation diagrams are plotted in Fig.5.4. All of the incompatible trace element-element variation diagrams illustrate slightly-to-well define positive trends between the Infranz volcanic plugs. These well-defined trends between those volcanic plugs are an indicator of the most probable formation of Infranz volcanic plugs from the same source of magmatic lineage. In all of the incompatible trace element-element variation diagrams the Lima Limo rhyolites tend to show their own distinct trends. The trace element variations between the Infranz volcanic plugs and the Lima Limo rhyolites are clearly observed; at a given concentration of Zr and Nb ppm (Fig 5.4A, D), the Infranz volcanic plugs tend to show higher Nb and Th ppm concentrations than the Lima Limo rhyolites respectively; on the other hand, the Lima Limo rhyolites tend to show higher concentrations of Y ppm at the given values of both Nb and La ppm than the Infranz volcanic plugs (Fig 5.4B, C). The noticeable differences in the concentrations of trace elements and the Lima Limo rhyolites form their own distinct trends suggest the most likely condition of the formation of these rocks from different source of magmatic lineage.

Incompatible trace element ratio-ratio, assumed to be not affected by fractional crystallization (Fig 5.4E) also support the above justification; in that incompatible trace element-element ratio ( $Zr/Th$  versus  $Zr/Nb$ ) for Lima Limo rhyolites and the Infranz volcanic plugs illustrate noticeable differences. These noticeable differences are the cause of most probably the source heterogeneity between the two rock suits. The Infranz volcanic plugs rather illustrate almost similar ratios in the  $Zr/Th$  versus  $Zr/Nb$  suggesting the most likely condition of formation of those volcanic plugs from the same magmatic lineage.

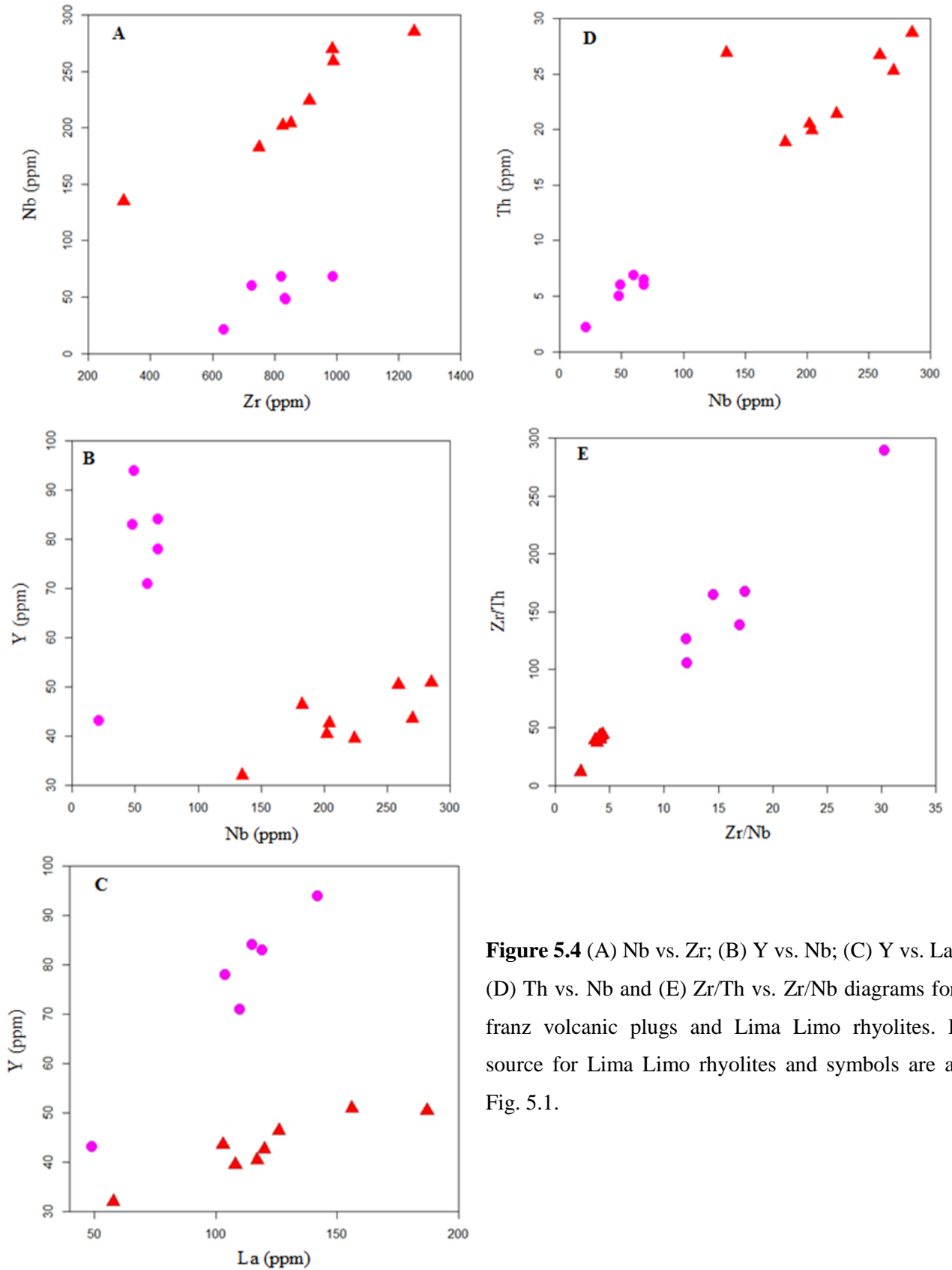


**Figure 5.4** (A) Nb vs. Zr; (B) Y vs. Nb; (C) Y vs. La; (D) Th vs. Nb and (E) Zr/Th vs. Zr/Nb diagrams for Infranz volcanic plugs and Lima Limo rhyolites. Data source for Lima Limo rhyolites and symbols are as in Fig. 5.1.

In chondrite-normalized rare earth element (REE) diagrams, the Infranz volcanic plugs (Fig. 5.5B) are characterized by strongly enriched light rare earth elements (LREEs) with  $[La/Yb]_N$  (8.97-21.66), on average (14.4). The samples from those volcanic plugs show parallel-to-subparallel REE patterns with relatively flat HREE patterns and almost similar negative Eu anomaly, except one sample (VP2-NG) which show strong fractionation in Eu (below 10). The parallel-to-subparallel chondrite-normalized REE patterns between the Infranz volcanic plugs and the negative Eu anomalies suggest the formation of those plugs by the same petrogenetic histories and controlled mainly by fractionation of feldspars respectively.

On the other hand, the chondrite –normalized rare earth element (REE) diagrams of the Infranz volcanic plugs and Lima Limo rhyolites (Fig.5.5A) illustrate almost similar, enriched light REE (LREEs) patterns, albeit differences in the sample/chondrite ratios of heavy REE (HREEs). Differences on the HREE patterns, but relatively flat in both cases, are observed between the Infranz volcanic plugs and Lima Limo rhyolites; the Infranz volcanic plugs show relatively lower sample/chondrite HREE ratios than Lima Limo rhyolites. The Chondrite normalized  $(La/Y)_N$  ratios of the Infranz volcanic plugs are higher than that of the Lima Limo rhyolites with  $(La/Y)_N$  ratios (7.79-10.29), on average (9.05). Both Lima Limo rhyolites and the Infranz volcanic plugs show negative Eu anomalies with Eu ( $Eu/Eu^* = 0.27- 0.90$ ), on average (0.46) and (0.43-0.83), (0.66) on average respectively. The negative Eu anomalies in both cases indicate the fractionation of feldspar from the system. There is some overlap in the Chondrite –normalized REE patterns between the Infranz volcanic plugs and the Lima Limo rhyolites. The difference in the sample/chondrite ratios of HREEs between the Infranz volcanic plugs and the Lima Limo rhyolites combined with the crossing patterns in the LREEs on the Chondrite –normalized REE diagrams suggest most probably the differences in the petrogenetic histories.

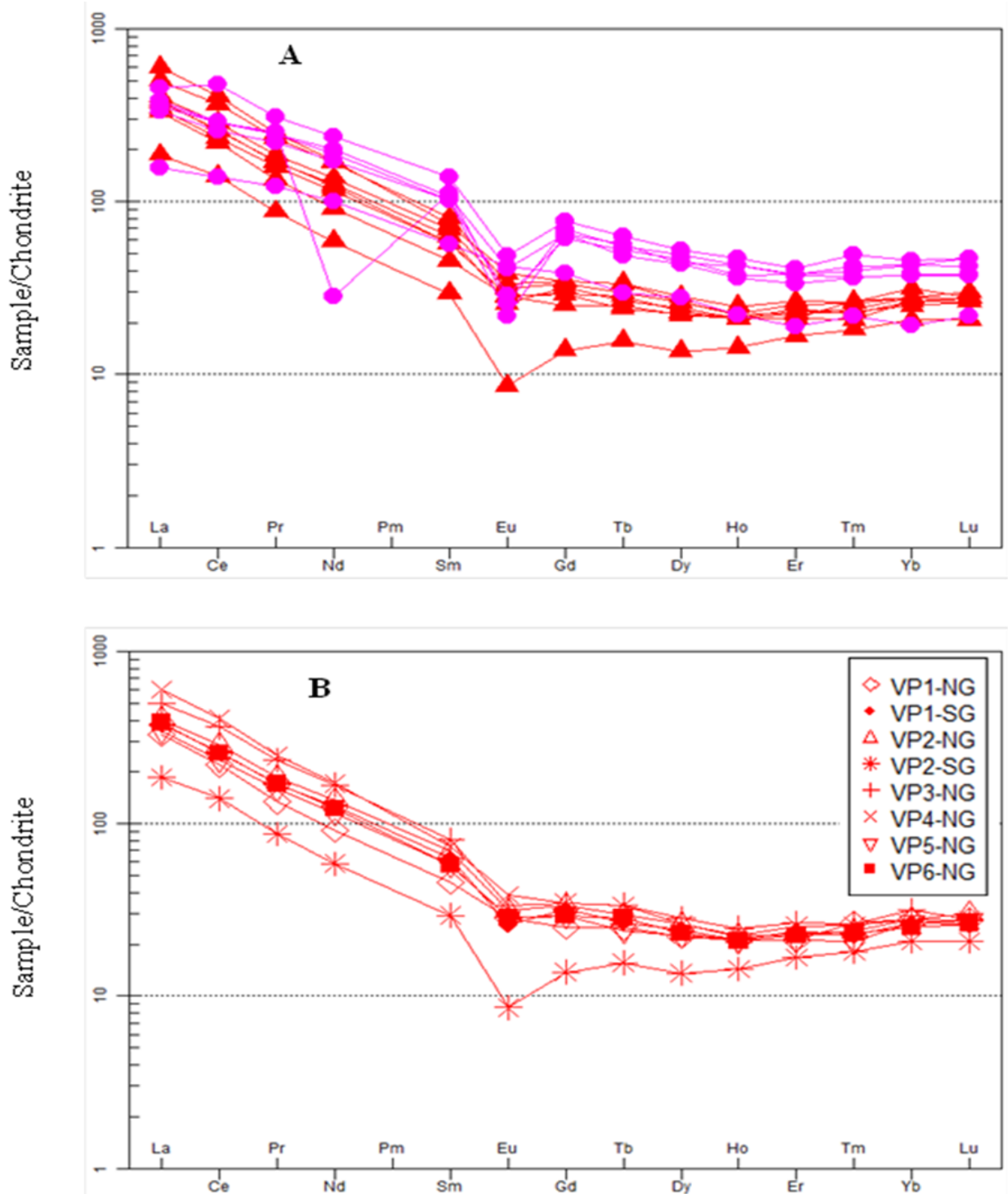


**Figure.5.5** Chondrite normalized REE plots (A) for the Infranz volcanic plugs and Lima Limo rhyolites and (B) for the Infranz volcanic plugs only. Normalization values are from Boynton (1984). Source of data and symbols for Fig. A are as in Fig 5.1.

Similarities, at same time differences are observed between the Infranz volcanic plugs and the Lima Limo rhyolites on the primitive mantle normalized multi- element plots (Fig 5.6A). Here the relations, on the basis of primitive mantle normalized multi-element plots, between these two rock types can be explained as: similarities that show positive (Rb, Zr and a little bit La and Nd) and negative (Ba, Sr, P and Ti) anomalies, almost similar sample/primitive mantle (K) ratios, relatively positive Pb anomalies for Lima Limo rhyolites and erratic concentrations for Infranz volcanic plugs, slightly positive Nb and Th (>100 times) and slightly negative (< 100 times) to that of chondrites for Infranz volcanic plugs and Lima Limo rhyolites respectively.

The negative anomaly in Ba and Sr indicates the fractionation of feldspar, P fractionation of apatite and Ti is due to Iron-Titanium oxide fractionation. The negative anomaly of Nb and Th in the Lima Limo rhyolites is an indicator of crustal contamination whereas, the absence of negative anomaly in Nb and Th in the Infranz volcanic plugs indicate no evidence of crustal contamination. The erratic behavior of Pb may be due to its mobility. The Infranz volcanic plugs act almost similarly except, one sample VP2-SG that illustrate the higher negative anomalies in Ba, Sr, P and Ti.

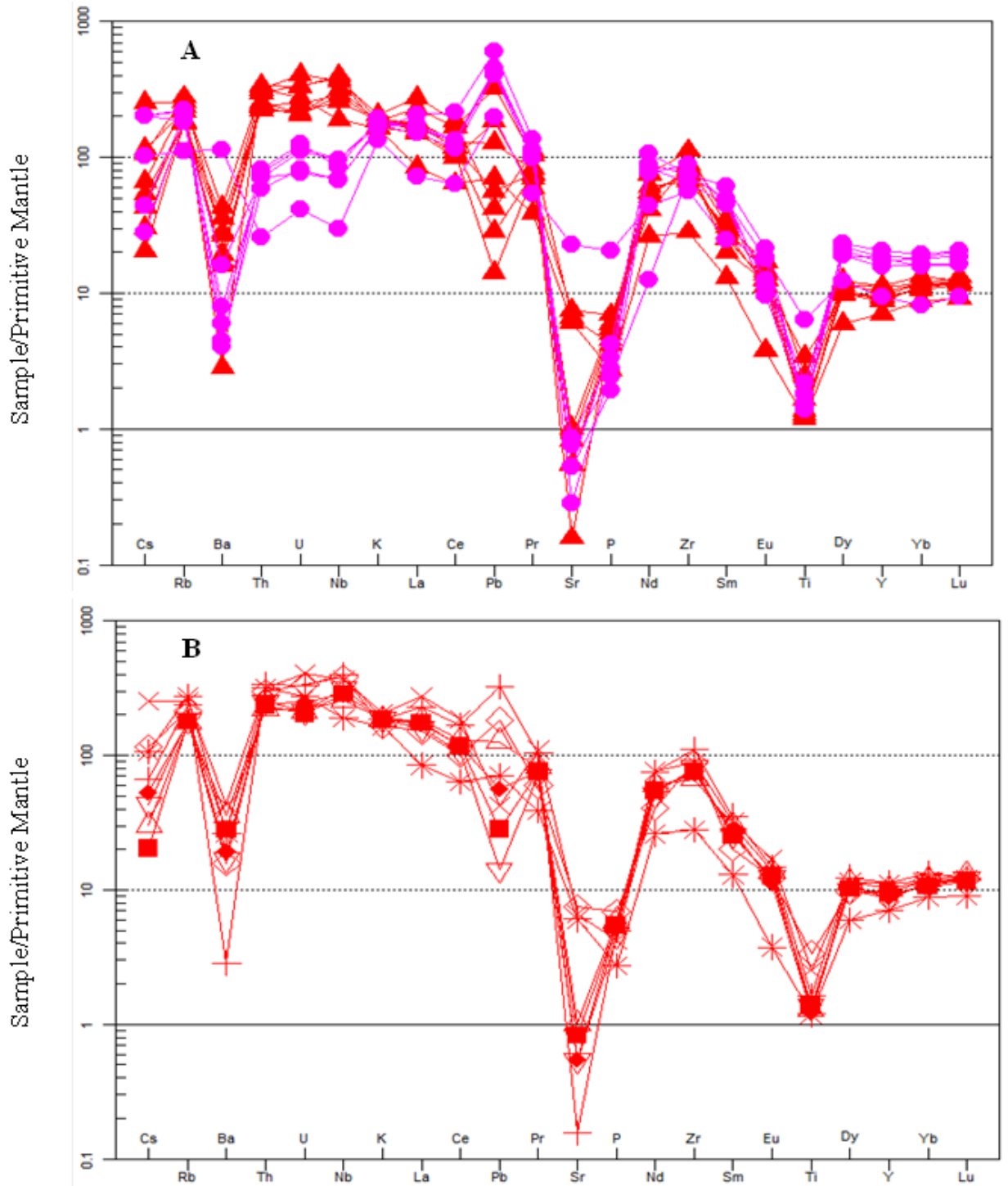


**Figure.5.6** Primitive mantle normalized incompatible, multi-element plots (A) for Infranz volcanic plugs and Lima Limo rhyolites and (B) for Infranz volcanic plugs only. Normalization values are from Sun and McDonough (1989). Source of data and symbols for A are as in Fig 5.1 and symbols for B are as in Fig 5.5B.

## **CHAPTER SIX**

### **6. DISCUSSION**

#### **6.1. Field, petrography and Geochemistry**

Volcanic plugs, fossil remains of innards of volcanoes, are thought to be the feeders of the surrounding volcanic rocks (<https://pubs.usgs.gov/gip/volc/structures.html>) at the time of their formation. Despite the feeding nature of volcanic plugs, the Infranz volcanic plugs are entirely surrounded by basaltic rocks, no any felsic volcanic rock nearby that gives an evidence of their feeding nature. This, the absence of felsic volcanic rocks around Infranz volcanic plugs, is probably due to the effect of erosion that may took felsic rocks fed by those volcanic plugs.

From field sample descriptions (Chapter Four), it is indicated that the compositionally phonolite-trachyte-rhyolite Infranz volcanic plugs (Fig 5.1) are dominantly characterized by the fine-grained textured groundmass with some medium-sized phenocrysts that range probably from nepheline (in VP4-NG), quartz (in VP2-SG) to alkali feldspar (in the rest of the samples). This field observation is consistent with petrography; petrographically most of the samples from the volcanic plugs of Infranz area show higher abundances of alkali feldspar, most importantly sanidine, which occur as phenocrysts, micro phenocrysts and the microlites of groundmass that oriented parallelly to subparallelly forming trachytic texture. This, the petrographically abundant alkali feldspar and trachytic texture, seems universal for the northern (e.g. Miruts Hagos et al., 2010, Natali et al., 2013) and north-western (e.g. Dercq et al., 2001, Daniel Meshesha and Shinjo, 2007) Ethiopian volcanic plugs. The abundant petrographic alkali feldspar nature of the Infranz volcanic plugs is also supported by: the high concentration (Table 5.1) of alkali element oxides Na<sub>2</sub>O (4.89-8.45 wt. %) and K<sub>2</sub>O (4.99-6.09 wt. %) in the geochemical analysis, the higher orthoclase and albite wt. % abundance in the CIPW normative mineralogy and the peralkaline character, which is manifested by the presence of normative acmite. The sample VP1-NG (Fig. 4.1), from the volcanic plug of Molalit, the plug found near Maksegnt,

contains coarse to medium grained, dark colored basaltic rock fragments that makes it exceptional than samples from other volcanic plugs. The presence of dark colored rock fragments in field observation of this sample is also manifested in geochemical analysis (Table 5.1), higher MgO, Fe<sub>2</sub>O<sub>3</sub>, Co and Cr, though not the lowest SiO<sub>2</sub>, concentrations relative to not only the volcanic plugs included in this study, but also the volcanic plugs of the northern (e.g. Miruts Hagos et al., 2010) and northwestern (e.g. Dercq et al., 2001) Ethiopia and in the CIPW normative mineralogy (Table 5.1), it is the only sample with normative olivine. However, these characteristics are not more consistent in the petrography, may be because of those rock fragments are excluded while thin section is prepared. According to (<https://pubs.usgs.gov/gip/volc/structures.html>), igneous materials in volcanic plugs may contain fragments and blocks of denser, coarse grained rocks higher in iron and magnesium, lower in silica, thought to be samples of Earth's deep crust or upper mantle. Thus, it is suggested that the materials of this plug may originate from deep within the earth.

## **6.2. Source Relations**

Incompatible trace element-element (Fig 5.4A to D) and trace element ratio-ratio (Fig 5.4 E) variation diagrams between Infranz volcanic plugs form slightly straight line, except in the Th versus Nb ppm (Fig 5.4D) diagram where the phonolitic plug show higher Th concentration than other trachyte-rhyolite volcanic plugs. The relatively straight line Infranz volcanic plugs form in trace element- element plots are best explained by the formation of those volcanic plugs from the same source. Another supportive evidence for the formation of the Infranz volcanic plugs from the same source is that the almost similar concentration of Zr/Th and Zr/Nb in the Zr/Th versus Zr/Nb diagram (Fig 5.4E). On most major element oxides versus silica variation diagrams (Fig. 5.2), the Infranz volcanic plugs and the Lima Limo rhyolites show different concentrations (e.g. TiO<sub>2</sub>, Al<sub>2</sub>O<sub>3</sub>, and CaO). Moreover, the Lima Limo rhyolites form their own distinct trends which in most cases not observed in samples of volcanic plugs rather, they cluster around the same point. The variations in concentration of major element oxides show the Infranz volcanic plugs and the Lima Limo rhyolites are also observed in trace elements (Fig. 5.3). In this variation diagram, Fig 5.3, the Infranz volcanic plugs tend to show higher (e.g. Nb) and lower (e.g. Yb) concentrations than the Lima Limo rhyolites at a given SiO<sub>2</sub> wt. %. The concentrations of trace elements between most of the volcanic plugs are clustered around the same point, as they do in major element oxides. Trace element- element and trace el-

ement ratio-ratio plots (Fig. 5.4) between the Infranz volcanic plugs and Lima Limo rhyolites best strengthen the concentration variations and distinct trends observed in Fig. 5.2 and 5.3. In most of this variation diagrams both Infranz volcanic plugs and the Lima Limo rhyolites form their own distinct trends with varying concentrations. The consistent variations in the concentration of major element oxides and trace elements observed tells that the Infranz volcanic plugs and the Lima Limo rhyolites are formed from different magmatic lineage.

The Infranz volcanic plugs, each other, form parallel to subparallel chondrite-normalized REE patterns (Fig 5.5B). As illustrated in this diagram the samples from those volcanic plugs show strong REE enrichment especially, the LREEs. They show relatively flat HREE patterns but, ten times greater than chondrites. This, 10 x greater concentration of samples from those volcanic plugs than chondrites, according to Wilson (1989) reveals the formation of those volcanic plugs from garnet free source.

### **6.3. Petrogenetic Processes**

On most of the major element oxide and trace element versus silica variation diagrams (Fig. 5.2 and 5.3) respectively, most of the samples from volcanic plugs of the Infranz area, are clustered around the same SiO<sub>2</sub> and also other major oxides (e.g. P<sub>2</sub>O<sub>5</sub>) and trace elements (e.g. Yb) concentrations. The clustering of SiO<sub>2</sub>, other major oxides and trace element concentrations around the same point in most of the samples may be due to the little effect of fractional crystallization on the formation of those volcanic plugs. The major element oxide and trace element versus silica variation diagrams (Fig. 5.2 and 5.3) respectively between the Infranz volcanic plugs and the Lima Limo rhyolites demonstrate that these suites of rocks are not related by simple suit-wide differentiation trends that can solely be explained by fractional crystallization. The major element variation diagrams (Fig 5.2): TiO<sub>2</sub>, CaO, Fe<sub>2</sub>O<sub>3</sub>t, Al<sub>2</sub>O<sub>3</sub> and Na<sub>2</sub>O versus SiO<sub>2</sub> wt. % and trace element variation diagrams (Fig 5.3): Nb, Th and Yb ppm versus SiO<sub>2</sub> wt. % clearly, though other variation diagrams are not too much discriminant, illustrate the difference between those two rock suits in that they are not related by fractional crystallization.

Both, the Infranz volcanic plugs and the Lima Limo rhyolites, on the chondrite-normalized RRE plots (Fig. 5.5A) show negative Eu anomaly. The negative Eu, (Eu/Eu\*=0.43-0.83) 0.66 on average, anomalies observed in the samples from those vol-

canic plugs suggests the fractionation of feldspar from the system (e.g. Wilson, 1989, Rollinson, 1993). Fractionations of other minerals in the formation of Infranz volcanic plugs are also observed on the primitive mantle normalized plots (Fig. 5.6B) in: Ba, due to the fractionation of K-feldspar, hornblende and biotite, in Sr due to the fractionation of plagioclase and K-feldspar (Wilson, 1989), in P due to fractionation of apatite and in Ti due to the fractionation of Fe-Ti oxides.

On the chondrite-normalized REE diagrams (Fig. 5.5B), the Infranz volcanic plugs form parallel-to-subparallel patterns. The parallel-to-sub parallel patterns between the Infranz volcanic plugs suggest the formation of those volcanic plugs by the same petrogenetic processes. On the contrary, the chondrite-normalized REE diagrams (Fig 5.5A) between the Infranz volcanic plugs and Lima Limo show crossing patterns. These crossing patterns on the chondrite-normalized diagram suggest the formation of the Infranz volcanic plugs and the Lima Limo rhyolites by different petrogenetic processes.

On the primitive mantle normalized incompatible, multi-element plots (Fig. 5.6 B), the Infranz volcanic plugs illustrate more or less similar patterns, nonetheless, the somehow unique behavior of the rhyolitic sample, because of it is more evolved, as observed in the chondrite-normalized REE plots (Fig 5.5B), with the exception of Pb which show erratic anomaly, may be due to its mobility. These similar patterns the volcanic plugs form supports the interpretation given for the chondrite-normalized plots. On the primitive mantle-normalized plots, it is evident that there is no (little) negative anomaly in Nb and Th between the Infranz volcanic plugs. The absence of negative anomalies in these elements suggests the free (little) crustal contamination formation of those volcanic plugs which is also observed in most of the northern (e.g. Miruts Hagos et al., 2010) and northwestern (e.g. Daniel Meshesha and Shinjo, 2007) Ethiopian volcanic plugs. The Lima Limo rhyolites form their own parallel trends and show crossing patterns with that of the Infranz volcanic plugs, as do in the chondrite-normalized REE plots. The crossing patterns the Lima Limo rhyolites form with the Infranz volcanic plugs strengthen the interpretation given in the chondrite-normalized REE patterns that those two rock suites are not formed by the same petrogenetic processes. Moreover, the relatively opposite, slightly positive to no (little) for Infranz volcanic plugs and negative for Lima Limo rhyolites, Th and Nb anomalies give a good supportive evidence as they pass through different petrogenetic histories. Note that, Dereje Ayalew et al. (2002) interpreted the negative Th and Nb anoma-

lies observed in the Lima Limo rhyolites as the contamination of parental magma by lower crust material.

#### **6.4. Comparison of Infranz and Previously Studied Volcanic Plugs**

Following the classification of northwestern Ethiopian continental flood basalt as high TiO<sub>2</sub> (HT) and low TiO<sub>2</sub> (LT) sub-provinces (Fig. 2.2) by Pik et al. (1998), Dereje Ayalew and Gezahegn Yirgu (2003) classified the felsic volcanic rocks of northwestern Ethiopia as high TiO<sub>2</sub> (HT) and low TiO<sub>2</sub> (LT) sub-provinces that follow similar trends as the flood basalt volcanics. According to these authors the HT felsic volcanic rocks (Wegel Tena rhyolites) have higher TiO<sub>2</sub> concentration (0.5-1 wt. %) whereas, the LT felsic volcanic rocks (Lima Limo rhyolites) have low TiO<sub>2</sub> concentrations (< 0.5 wt. %). The Infranz volcanic plugs geographically are grouped under the LT sub provinces of basaltic and felsic volcanic rocks. Of the studied eight samples, two (VP1-NG and VP2-NG) show higher TiO<sub>2</sub> concentrations (> 0.5 wt. %), which is proposed by Dereje Ayalew and Gezahegn Yirgu (2003) for high TiO<sub>2</sub> felsic volcanic rocks (Wegel Tena rhyolites). This higher value of TiO<sub>2</sub> concentrations in the two samples of Infranz volcanic plugs are comparable with the two samples (98-100 and 98-101) of Dercq et al (2001) around Amed Ber (Fig. 4.1). Other six samples show lower TiO<sub>2</sub> concentrations (< 0.5 wt. %) as Dereje Ayalew and Gezahegn Yirgu (2003) proposed for low TiO<sub>2</sub> felsic volcanic rocks (Lima Limo Rhyolites), but generally are greater than the northern Ethiopian phonolite-trachyte volcanic plugs (Miruts Hagos et al., 2010, Natali et al., 2013) and the volcanic plug from Simien shield (Dercq et al., 2001). The Axum-Adwa- and the Simien volcanic plugs show lower TiO<sub>2</sub> (generally < 0.15 Wt. %) concentrations (Fig 6.1) than all the volcanic plugs included under this study (generally > 0.26 wt. %). This suggests the lower TiO<sub>2</sub> concentrations of Axum-Adwa- including Simien volcanic plugs, though the difference is not too much as proposed by Pik et al. (1998) for basalts and Dereje Ayalew and Gezahegn Yirgu (2003) for rhyolites, than the northwestern Ethiopian volcanic plugs.

The TiO<sub>2</sub> concentration differences in the northern and northwestern Ethiopian volcanic plugs are also observed in some selected trace element- element (Fig 6.2A, B) and trace element ratio-ratio plots (Fig 6.2C, D). On the Nb versus Zr (ppm) diagram (Fig 6.2A), the volcanic plugs of northern and northwestern Ethiopia form a slight straight line with high concentration of Nb in the Addis Zemen volcanic plug and low in the Amed Ber

volcanic plug and slightly low in the Adwa volcanic plugs. The Y versus Nb (ppm) diagram (Fig 6.2B) is rather somehow discriminant; Axum-Adwa volcanic plugs tend to show higher concentrations of Y than the Infranz and Addis Zemen volcanic plugs which tend to show the lowest concentration of Y.

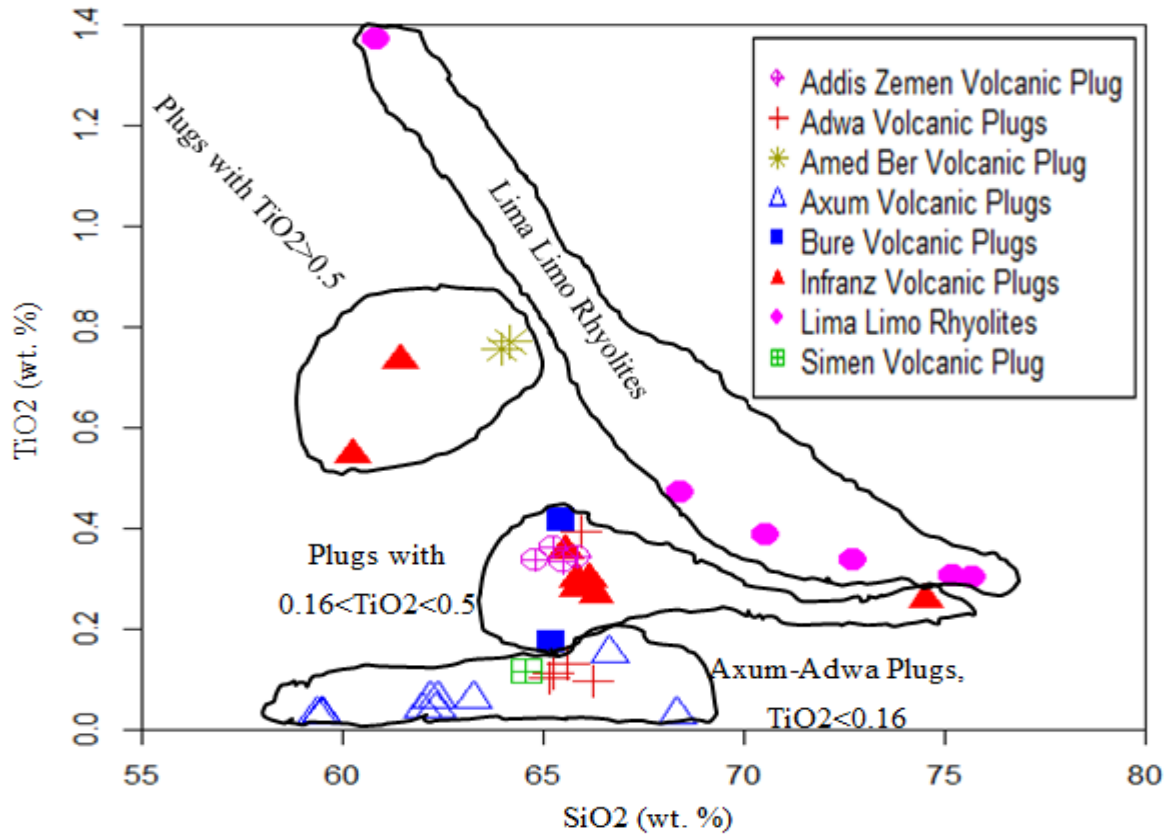


**Figure 6.1** TiO<sub>2</sub> versus SiO<sub>2</sub> (wt. %) variation diagram for the northern and northwestern Ethiopian volcanic plugs and that of the Lima Limo rhyolites. Data are from Miruts et al. (2010); Natali et al. (2013); Dercq et al. (2001); Daniel Meshesha and Shinjo (2007) for volcanic plugs and Dereje Ayalew and Gezahegn Yirgu (2003) for Lima Limo rhyolites.

The two ratio diagrams (Fig 6.2C, D) support the difference in the concentration of TiO<sub>2</sub> concentration between the northern and northwestern volcanic plugs. Nb/Y versus Ti/Zr diagram (Fig 6.2C) illustrates the lowest Nb/Y and Ti/Zr ratios of Axum-Adwa volcanic plugs, the intermediate ratio of Infranz volcanic plugs and the relatively highest Ti/Zr ratio of Amed Ber volcanic plug. On the contrary, Addis Zemen and Simien volcanic plugs tend to show the highest ratio of Nb/Y. The Nb/Y versus Rb/Y (Fig 6.2D) diagram also support the ratio diagram Nb/Y versus Ti/Zr. Axum-Adwa volcanic plugs show the lowest, but, greater than the Lima Limo rhyolites, Nb/Y and Ti/Zr ratios followed by the Infranz volcanic plugs and finally, highest ratio, Addis Zemen and Simien volcanic plugs.

The difference in the TiO<sub>2</sub> concentration, Nb/Y, Ti/Zr and Rb/Y ratios and the slight-to no trend the northern and northwestern Ethiopian volcanic plugs form in the Nb versus Zr and Y versus Nb diagrams may be due to the source heterogeneity.

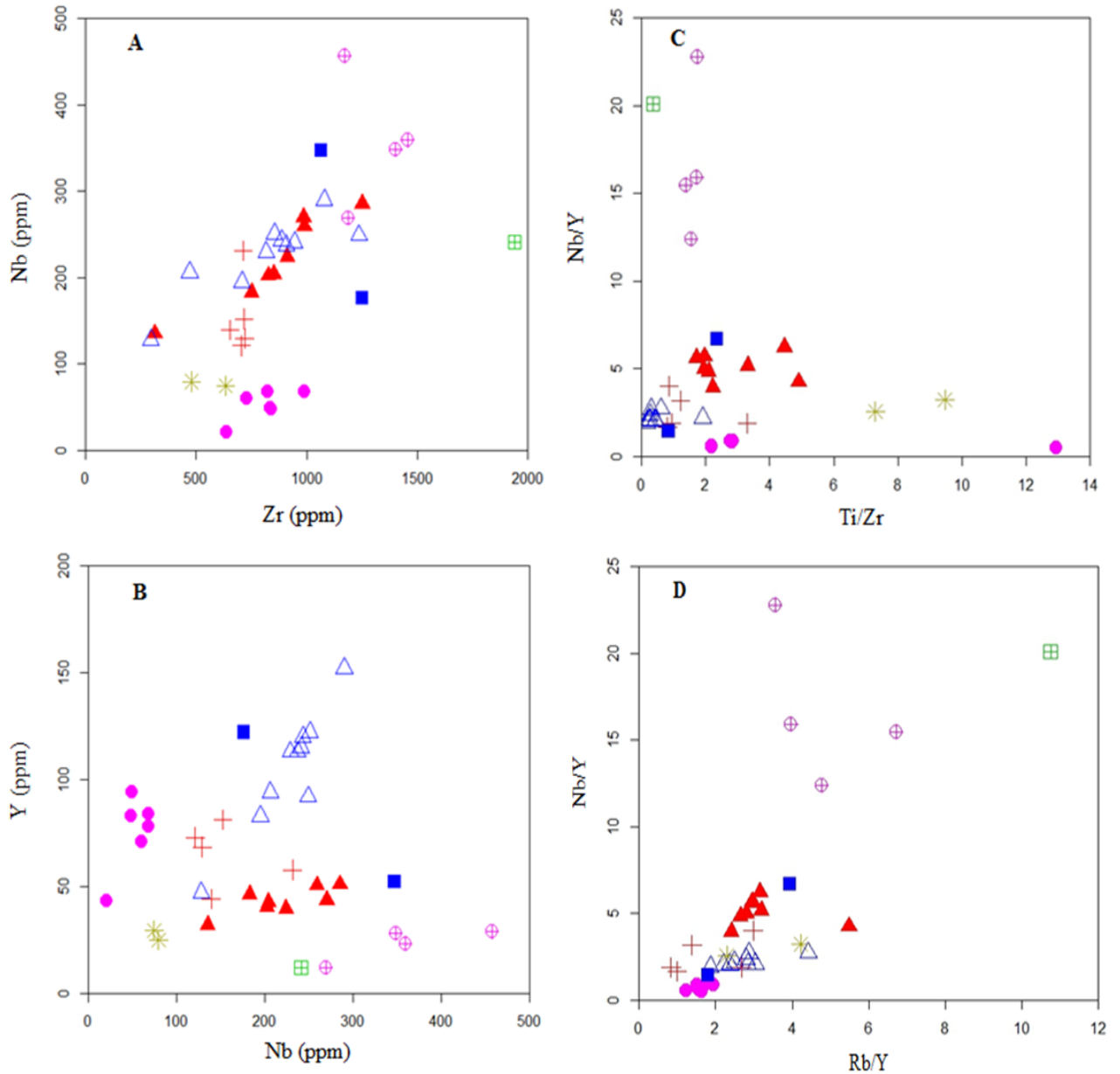


**Figure 6.2** (A) Nb vs. Zr (B) Y vs. Nb (C) Nb/Y vs. Ti/Zr and (D) Nb/Y vs. Rb/Y diagrams for the northern and northwestern Ethiopian volcanic plugs and that of the Lima Limo rhyolites. Data sources and symbols are as in Fig. 6.1.

## **CHAPTER SEVEN**

### **7. CONCLUSION AND RECOMMENDATION**

#### **7.1. Conclusion**

Volcanic plugs of the Infranz area, northwestern Ethiopia, projects an estimated 200-300 meters from the present erosional basaltic surface with 120-200 meters of width. They are entirely surrounded by the basaltic rocks, may be because of the eroded away of felsic volcanic rocks that are thought to be fed by those volcanic plugs. Most of those volcanic plugs are characterized by fine grained, pale colored with sparsely distributed medium grained alkali feldspar phenocrysts; petrographically those samples show considerable amounts of alkali feldspar in trachytes, nepheline in phonolite and quartz phenocrysts in rhyolite plugs set in fine grained parallelly aligned alkali feldspar and plagioclase groundmass which is an indicator of the formation of those volcanic plugs while magma is flowing.

Volcanic plugs of the Infranz area, northwestern Ethiopia ranges in composition from phonolite through trachyte to rhyolite that plots in the alkaline region. Of the studied eight volcanic plugs, six are trachytic in composition and the remaining two are phonolite and rhyolite. Major- and trace-element concentrations of the Infranz volcanic plugs show clustering around the same point which is explained by the little effect of fractional crystallization in the formation of those volcanic plugs. The majority of volcanic plugs of the study area are silica saturated peralkaline rocks characterized by the absence of modal, but, normative quartz.

On the chondrite-normalized REE plots volcanic plugs of the Infranz area are characterized by highly fractionated REEs  $[La/Yb]_N$  (8.97-21.66), LREEs  $[La/Sm]_N$  (5.87-7.26) with negative Eu ( $Eu/Eu^* = 0.43-0.83$ ) anomaly; the primitive mantle-normalized plots illustrate positive in the incompatible trace elements: Rb, Th, Nb, La, Nd and Zr, negative in the Ba, Sr, P and Ti and erratic in Pb anomalies.

From major element oxide and trace element versus silica variation diagrams in combination with chondrite-normalized REE and primitive mantle normalized incompatible, multi-element plots the following conclusions are drawn: volcanic plugs of the Infranz area, northwestern Ethiopia are formed from the same, garnet free source by the same petrogenetic process with little role of fractional crystallization between them and are free (little) crustal contamination involvement in their formation and the Lima Limo rhyolites are compositionally distinct from those of the Infranz volcanic plugs, implies the Infranz volcanic plugs are not the feeders for the Lima Limo rhyolites.

## **7.2. Recommendation**

There is no well-defined age data for the volcanic plugs of the northern and northwestern Ethiopian volcanic plugs except the one by Natali et al. (2013), therefore it is better to have a good age record for those volcanic plugs to well understand their age relationship with the Ethiopian continental flood basalt.

The difference in the TiO<sub>2</sub> concentration, Nb/Y, Ti/Zr, Nb/Y and Rb/Y ratios, though from slight observation, between the northern and northwestern Ethiopian volcanic plugs needs detail study to put any justification for this simple observation.

Isotopic data are also not documented in an adequate amount for the northwestern Ethiopian volcanic plugs which also are recommended for volcanic plugs of the present study to further constrain the source regions.

## REFERENCES

- Begosew Abate, Koiberl, C., Buchanan, P. C. and Korner, W. (1998). Petrography and geochemistry of basaltic and rhyodacitic rocks from Lack Tana and Gimjabet-Kosober areas (North Central Ethiopia). *Journal of African earth sciences*. **26**:119-134.
- Berhe, S. M., Desta, B., Nicoletti, M. and Tefera, M. (1987). Geology, geochronology and geodynamic implications of the Cenozoic magmatic province in W and SE Ethiopia. *Journal of Geological Society, London*. **144**:213-226.
- Boynton, W. V. (1984). Cosmochemistry of the rare earth elements: meteorite studies. In: Henderson P. (ed.), *Rare earth element geochemistry*. Elsevier, New York.
- Daniel Meshesha and Shinjo, R. (2007). Crustal contamination and diversity of magma sources in the northwestern Ethiopian volcanic province. *Journal of mineralogical and petrological sciences*. **102**: 272-290.
- Daniel, C. (2009). Heterogeneous initial Sr isotope compositions of highly evolved volcanic rocks from the Main Ethiopian Rift, Ethiopia. *Bull Volcanol*. **71**:495–508.
- Davidson, A. (1980). Age of volcanism and rifting in southwestern Ethiopia. *Nature*. **283**: 657-658.
- Davidson, A. (1983). Reconnaissance geology and geochemistry of parts of Illubabur, Kafa, Gemu Gofa and Sidamo, Ethiopia. E.I.G.S,Bull.No.2, Addis Ababa, Ethiopia.
- Dercq, M., Arndt, N., Lapierre, H. and Gezahegn Yirgu. (2001). Les pitons volcaniques d'Éthiopie sont les conduits d'alimentation des trachytes des volcans boucliers. *C. R. Acad. Sci. Paris, Sciences de la Terre et des planets*. **332**:609–615.
- Dereje Ayalew, Barbey, P., Marty, B., Reisberg, L., Gezahegn Yirgu and Pik, R. (2002). Source, genesis, and timing of giant ignimbrite deposits associated with Ethiopian continental flood basalts. *Geochemica et Cosmochemica Acta*. **66**:1429-1448.

- Dereje Ayalew and Gezahegn Yirgu. (2003). Crustal contribution to the genesis of Ethiopian plateau rhyolitic ignimbrites: basalt and rhyolite geochemical provinciality. *Journal of the Geological Society, London*. **160**: 47–56.
- Dereje Ayalew, Marty, B, Barbey, P, Gezahegn Yirgu and Endale Ketefo. (2006). Sub lithospheric source for Quaternary alkaline Tepi shield, southwest Ethiopia. *Geochemical Journal*. **40**: 47-56.
- Dereje Ayalew and Gibson, S.A. (2009). Head- to- tail transition of the Afar mantle plume: Geochemical evidence from a Miocene bimodal basalt-rhyolite succession in the Ethiopian Large Igneous Province. *Lithos*. **112**:461-476.
- Dereje Ayalew. (2011).The relations between felsic and mafic volcanic rocks in continental flood basalts of Ethiopia: implication for the thermal weakening of the crust. *Geological Society, London, Special Publications*. **357**. 253-264.
- Ebinger, C.J., Yemane,T., Woldegabriel,G., Aronson, L.J. and walter, C.R. (1993). Late Eocene-Recent volcanism and faulting in the southern main Ethiopian rift. *Journal of the Geological Society, Geological Society of London*. **150**: 99-108.
- Furman, T. (2007). Geochemistry of East African Rift basalts: An overview. *Journal of African Earth Sciences* **48**: 147–160.
- Furman, T., Nelson, W.R., Linda, T. and Elkins-Tanton. (2016) Evolution of the East African rift: Drip magmatism, lithospheric thinning and mafic volcanism. *Geochimica et Cosmochimica Acta* **185**: 418–434.
- Gates, A. E. and Richie, D. (2007). *Encyclopedia of earthquakes and volcanoes*, 3rd ed. Facts on file.365pp.
- George, R.M., Rogers, N. and Kelley, S. (1998). Earliest magatism in Ethiopia: Evidence for two mantle plumes in one flood basalt province. *Geology*. **26**: 923–926.
- Gill, R. (2010). *Igneous Rocks and Processes, A Practical Guide*. Wiley-Blackwell, Malaysia, 472pp.

Hofmann, C., Courtillot, V., Feraud, G., Rochette, P., Gezahegn Yirgu., Ketefo, E. & Pik, R. (1997). Timing of the Ethiopian flood basalt event and implications for plume birth and global Change. *Nature*. **389**: 838-841.

<https://en.climate-data.org/location/1183/> accessed on 12.02.2018.

<https://pubs.usgs.gov/gip/volc/structures.html> accessed on 12.01.2018.

Janousek, V., Farrow, M. C. and Erban, V. (2006). Interpretation of whole-rock geochemical data in igneous geochemistry: introducing Geochemical Data Toolkit (GCD-kit) 4.1. *Journal of Petrology* **47** (6): 1255-1259.

Kazmin, V. (1975). Explanation of the Geological map of Ethiopia. Ministry of Mines, Energy and Water resource, Geological survey of Ethiopia. 18pp.

Kieffer, B., Arndt, N., Lapierre, H., Basitien, F., Bosch, D., Pecher, A., Gezahegn Yirgu., Dereje Ayalew., Weis, D., Gerram, D.A., Keller, F & Meugniot, C. (2004). Flood and shield basalts from Ethiopia: Magmas from the African Superswell. *J. Petrology*. **45**: 793-834.

Le Bas, M. J., Le Maitre, R.W., Streckeisen, A. and Zanettin, B. (1986). A chemical classification of volcanic rocks based on the total alkali-silica diagram. *Journal of Petrology*. **27**: 745-750.

Lowenstern, J. (2000). CIPW NormCac\_JBL.xls, United States Geological Survey.

Macdougall, D.J. (1988). *Continental flood basalts. Petrology and structural geology*. 344pp.

Marty, B., Pik, R. and Gezahegn Yirgu. (1996). Helium isotopic variations in Ethiopian plume lavas: nature of magmatic sources and limit on lower mantle contribution. *Earth and Planetary Science Letters*. **144** : 223-237.

Mengesha Tefera, Tadiwos Chernet and Workineh Haro (1996). Exploration of the geological map of Ethiopia (1:20,000,000), 3<sup>rd</sup> ed., Ethiopian institutes of geological surveys. Unpublished technical report, Addis Ababa, Ethiopia. 83pp.

- Merla, G., Abate, E., Azzaroli, A., Bruni, P., Caunti, P., Fazzuoli, M., Sagri, M. and Taccioni, P. (1979). Geological map of Ethiopia and Somalia (1973):1:2,000,000 and comment with major land forms. 98pp.
- Minyahl Teferi, Dereje Ayalew, Ishiwatari, A, Arai, S and Akihiro, T. (2014). Ferropicrite from the Lalibela area in the Ethiopian large igneous province. *Journal of Mineralogical and Petrological Sciences*. **109**:191-207.
- Miruts Hagos, Koeberl, C, Vries, W.B. (2016) The Quaternary volcanic rocks of the northern Afar Depression (northern Ethiopia): Perspectives on petrology, geochemistry, and tectonics. *Journal of African Earth Sciences*. **117**: 29-47.
- Miruts, Hagos , Koeberl, C. , Kabeto, K. and Koller, F. (2010). Geochemical characteristics of the alkaline basalts and the phonolite –trachyte plugs of the Axum area, northern Ethiopia. *Austrian Journal of Earth Sciences*. **103/2** : 153-170.
- Mohr, P. (1983). Ethiopian flood basalt province. *Nature*. **303**:577–584.
- Mohr, P., Zanettin, B., (1988). The Ethiopian flood basalt province. In *Continental flood basalts* McDougall, J.D. (Ed.),. Kluwer Acad. Publ., Dordrecht. 63-110.
- Mulugeta Alene, Hart, W. K, Saylor, B.Z, Deino, A, Mertzman, S, Yohannes Haile-Selassie and Gibert, L.B. (2017). Geochemistry of Woranso–Mille Pliocene basalts from west-central Afar, Ethiopia: Implications for mantle source characteristics and rift evolution. *Lithos*. **282-283**. 187-200.
- Natali, C., Beccaluva, L., Bianchini, G. and Siena, F. (2011). Rhyolites associated to Ethiopian CFB: Clues for initial rifting at the Afar plume axis. *Earth and Planetary Science Letters*. **312**: 59-68.
- Natali, C., Beccaluva, L., Bianchini, G., and Siena, F. (2013). The Axum–Adwa basalt–trachyte complex: a late magmatic activity at the periphery of the Afar plume. *Contrib Mineral Petro*, Springer-Verlag Berlin Heidelberg. **370**: 166:351.
- Philpotts, A.R. (2003). *Petrography of Igneous and Metamorphic Rocks*. Waveland press, INC, United States of America, 190pp.

- Pik, R., Deniel, C., Coulon, C., Gezahegn Yirgu and Marty B. (1999). Isotopic and trace element signatures of Ethiopian flood basalts: Evidence for plume–lithosphere interactions. *Geochimica et Cosmochimica Acta*. **63**: 2263–2279.
- Pik, R., Deniel, C., Coulon, C., Gezahegn Yirgu, Hofmann, C. and Dereje Ayalew (1998). The Northwest Ethiopian plateau flood basalts: classification and spatial distribution of magma types. *Journal of Volcanology and Geothermal Research*. **81**: 91–111.
- Prave, R. A., Bates, R. C., Donaldson, H.C., Toland, H., Condon, J.D., Mark, D. and Raub, D.T. (2016). Geology and geochronology of the Tana Basin, Ethiopia: LIP volcanism, super eruptions and Eocene-Oligocene environmental change. *Earth and Planetary Science Letters*. **443**: 1-8.
- Rochette, P., Tamrat, E., Fe´raud, G., Pik, R., Courtillot, V., Ketefo, E., Coulon, C., Hofmann, C., Vandamme, D., and Gezahagh Yirgu. (1998). Magnetostratigraphy and timing of the Oligocene Ethiopian traps. *Earth Planet. Sci. Lett.* **164**:497–510.
- Rollinson, H.R. (1993). *Using geochemical data: evaluation, presentation, interpretation*. Pearson prentice hall, England. 380pp.
- Rooney, T.O., Hart, W. T., Hall, C. M., Dereje Ayalew Ghiorso, S.M., Hidalgo, P. and Gezahegn Yirgu. (2012). Peralkaline magma evolution and the tephra record in the Ethiopian Rift. *Contrib Mineral Petrol*. **164**:407–426.
- Rooney, T.O, Nelson, W.R, Dereje Ayalew, Hanan, B, Gezahegn Yirgu and Kappelman, J. (2017b). Melting the lithosphere: Metasomes as a source for mantle-derived Magmas. *Earth and Planetary Science Letters*. **461**:105-118.
- Rooney, T.O, Lavigne, A, Svoboda, C, Girard, G, Gezahegn Yirgu, Dereje Ayalew and Kappelman, J. (2017a). The making of an underplate: Pyroxenites from the Ethiopian lithosphere. *Chemical Geology*. **455**: 264-281.
- Sun, S.S., McDonough, W.F.(1989).Chemical and isotopic systematics of oceanic basalts: Implications for mantle composition and processes. In: *Sunders, A.D. and Norry,*

M.J. (Ed.), *Magmatism in the ocean basins*. Geological Society of London. **42**: 313–345.

Williams, F.M. (2016). *Understanding Ethiopia Geology and scenery, GeoGuide*. Springer International Publishing, Switzerland, 356pp.

Wilson, M. (1989). *Igneous Petrogenesis: A Global Tectonic Approach*. Springer, Netherlands. 480pp.

Zanettin, B. Visentin, J. E. and Piccirillo, E. M. (1978). *Volcanic succession, tectonics and Magmatology in central Ethiopia*. Padova, Societa Cooperativa tipografica. 16pp.

## **APPENDIX I**

### **SECONDARY GEOCHEMICAL DATA**

Geochemical analysis results of Lima Limo rhyolites used in plots, from Dereje Ayalew and Gezahegn Yirgu (2003).

Sample:	98-139	98-150	98-149	98-162	AD 26	98-138
SiO <sub>2</sub>	58.9	65.5	67.2	69.4	74.1	75.0
TiO <sub>2</sub>	1.33	0.45	0.37	0.32	0.30	0.30
Al <sub>2</sub> O <sub>3</sub>	15.0	13.3	12.7	12.5	12.4	11.8
Fe <sub>2</sub> O <sub>3</sub> *	7.8	6.3	5.0	3.9	2.3	2.9
MnO	0.16	0.17	0.15	0.09	nd	0.21
MgO	1.77	0.21	0.12	0.12	nd	0.08
CaO	4.21	1.26	1.20	0.90	0.39	0.10
Na <sub>2</sub> O	3.3	3.6	3.3	2.6	4.0	3.8
K <sub>2</sub> O	3.9	4.9	5.2	5.6	5.0	4.8
P <sub>2</sub> O <sub>5</sub>	0.43	0.07	0.05	0.04	0.06	0.09
LOI	3.2	4.3	4.6	4.4	1.0	0.9
Total	99.98	99.91	99.88	99.87	99.55	99.98
Ba	787	56	42	28	31	113
Cs	0.8	1.6	1.6	1.6	0.35	0.22
Ga	24	28	27	30	35	32
Hf	15	25	23	21	23	22
Nb	21	68	68	60	48	49
Pb	14	29	32	30	32	43
Rb	70	118	143	138	129	116
Sr	484	18	16	11	6	11
Ta	1.3	4.0	4.2	3.7	3.2	2.9
Th	2.2	6.0	6.5	6.9	5	6
U	0.87	2.31	2.49	2.65	1.7	1.6

Y	43	78	84	71	83	94
Zr	636	988	821	728	837	833
La	49	104	115	110	119	142
Ce	112	207	232	233	237	384
Pr	15	27	31	30	30	38
Nd	60	104	17	113	120	144
Sm	11	20	22	20	21	27
Eu	3.1	2.1	1.9	1.6	3.0	3.6
Gd	10	16	18	17	17	20
Tb	1.4	2.5	2.6	2.3	2.7	3.0
Dy	9	15	16	14	14	17
Ho	1.6	2.7	3.1	2.6	3.1	3.4
Er	4	8	8	7	7.8	8.6
Tm	0.71	1.28	1.38	1.17	1.2	1.6
Yb	4	9	9	8	7.8	9.5
Lu	0.70	1.36	1.51	1.20	1.22	1.52

## **APPENDIX II**

### **ABBREVIATIONS**

Ab= Albite

Ac= Acmite

An= Anorthite

Ap= Apatite

C= Corundum

Di= Diopside

Fig. = Figure

Hm= Hematite

HREEs= Heavy Rare Earth Elements

Hy= Hypersthene

Il= Ilmenite

LRREs=Light Rare Earth Elements

Mt= Magnetite

Ne= Nepheline

Ol= Olivine

Or= Orthoclase

Pf= Perovskite

PPL=Plane Polarized light

Q=Quartz

REE= Rare Earth Element

Ru= Rutile

Tn= Titanite

Vs. =Versus

Wo= Wollastonite

Wt. % = Weight percent

XPL= Cross Polarized Light